Supplementary Information

Imipridone anticancer compounds ectopically activate the ClpP protease and represent a new scaffold for antibiotic development

Samuel Jacques[1]*, Almer M. van der Sloot[1]*, Caroline Huard[1]*, Jasmin Coulombe-Huntington[1], Sarah Tsao[1], Sylvain Tollis[1], Thierry Bertomeu[1], Elizabeth J. Culp[2], Daniel Pallant[2], Michael A. Cook[2], Eric Bonneil[1], Pierre Thibault[1], Gerard D. Wright[2] and Mike Tyers[1]

[1]Institute for Research in Immunology and Cancer, University of Montréal, Montréal, Quebec, Canada

[2]David Braley Center for Antibiotic Discovery, Michael G. DeGroote Institute for Infectious Disease Research, Department of Biochemistry and Biomedical Sciences, McMaster University, Hamilton, Ontario, Canada

*these authors contributed equally to this work

correspondence: am.van.der.sloot@umontreal.ca; md.tyers@umontreal.ca; tel 514-343-6668

This file contains:

Supplementary Table S1, S2 and S3 in Excel format are provided via figshare

Supplementary Methods

Chemicals. ONC201 (TIC10) (HY-15615A), ONC212 (HY-111343), TIC10-isomer (HY-15615), ethambutol (HY-B0535), rifampin (HY-B0272), isoniazid (HY-B0329) and vancomycin (HY-17362) were obtained from MedChemExpress. Doxycycline (D9891), streptomycin (S6501) and tetracycline (T3383) were from Sigma. Ciprofloxacin (61-277-RF) was from Corning Life Science. Other compounds and reagents were from Sigma unless otherwise stated. All compounds were dissolved in DMSO (Corning, 25-950-CQC), except for streptomycin, which was dissolved in water.

Cell lines and culture conditions. The HEK293T (CRL-3216) cell line was purchased from ATCC, the NALM-6 cell line was provided by Dr. Steven Elledge (Harvard Medical School, Boston, Massachusetts, USA) and the RPE1-hTert cell line was provided by Daniel Durocher (Lunenfeld-Tanenbaum Research Institute, Toronto, Ontario, Canada). NALM-6 cells were grown in Roswell Park Memorial Institute (RPMI) 1640 Medium (Wisent, 350-000-CL) supplemented with 10% Fetal Bovine Serum (FBS) (v/v) (Sigma, F1051). HEK293T and RPE1-hTert cells were cultured in Dulbecco's Modified Eagle Medium (DMEM) (Wisent, 319-005-CL) supplemented with 10% FBS (v/v). The clonal NALM-6 cell line #20 that bears an integrated doxycycline-inducible allele of Cas9 used for the CRISPR knockout screen has been previously described (BERTOMEU *et al.* 2018). All cells were incubated at 37°C in a humidified atmosphere containing 5% CO_2 and maintained in exponential growth phase by sub-culturing 3 times per week. NALM-6 and RPE1-hTert cell lines were confirmed to be mycoplasma-negative by standard multiplex PCR.

Proliferation dose-response curves. A 10-point titration curves of ONC212 or ONC201 ranging from 2.5 nM to 50 µM in quadruplicate were prepared in 384-well plates using an Echo 555 Acoustic liquid handler robot (Labcyte, San Jose, California, USA). For determination of the IC_{50} values for genome-wide CRISPR knockout screens, the inducible Cas9 NALM-6 cell line was plated at a density of 200,000 cells/mL in 50 µL medium/well. For analysis of CLPP and MIPEP depletion effects on ONC212 and ONC201 resistance, RPE1-hTert-shCLPP and NALM-6-sgRNA-CLPP or sgRNA-MIPEP populations were plated at a density of 1,000 and 10,000 cells/well,

respectively, in 50 µL medium/well. After 72 h, cell proliferation was assessed by CellTiter-Glo Luminescent Cell Viability Assay (Promega, G7573). Statistical analysis was performed using IDBS Activity Base (IDBS, Boston, Massachusetts, USA). All experiments were run in duplicate or triplicate and cell viability was expressed as a percentage compared to the vehicle DMSO control.

Genome-wide pooled CRISPR library knockout screens. A NALM-6 clone with an inducible allele of Cas9 that had been previously transduced with the 278,000 member EKO sgRNA library was used to perform the genome-wide knockout screens (BERTOMEU *et al.* 2018). The frozen uninduced library pool was thawed in RPMI 1640 media containing 10% FBS (v/v) and Cas9 expression was induced with doxycycline (Sigma, D9891) at 2 µg/mL. After 8 days of doxycycline treatment, the pooled library was split in different T-75 flasks (28 million cells per flask, corresponding to ~100 cells/sgRNA for the 278,754 different sgRNAs in the EKO library) at 400,000 cells/mL. Compounds (150 nM ONC212, 10 µM ONC201 or DMSO only) were added from 1000X stocks to a final DMSO concentration of 0.1% (v/v). Cells were counted every 2 days using a Beckman Coulter Z2 Cell Counter (Beckman Coulter, Brea, California, USA) for a total of 8 days. Once cultures reached 800,000 cells/mL, 28 million cells were seeded into fresh medium at 400,000 cells/mL with fresh compound. Otherwise, the incubation of the cells was continued for a further 2 days. Compound concentrations were chosen to result in an intermediate growth inhibition (approximately IC'_{50} value) of NALM-6 cells. After compound treatment, cells were collected and genomic DNA extracted using a Gentra Puregene Cell Kit (Qiagen, 158745). The sgRNA library was amplified from 184.8 µg of genomic DNA (corresponding to 28 million cells, given that a human diploid cell contains 6.6 pg DNA) in a first round of PCR with 57.5 U of Green Taq DNA polymerase (GenScript, E00043), 0.2 mM dNTP mix (GenScript, C01582) and 0.4 µM each of outer primer 1 and 2 (Supplementary Table S4), in a total volume of 2.3 mL. Multiple 100-µL reactions were set up in 96-well format on a T100 thermal cycler (BioRad, Hercules, California, USA) with a program of 5 min at 95°C, followed by 25 cycles of 35 sec at 94°C, 50 sec at 52°C and 40 sec at 72°C, and a final step of 10 min at 72°C after the last cycle. Reaction mixes were pooled and the presence of a 475 bp amplicon was verified by DNA

electrophoresis. A second PCR reaction with 10 µL of 1:20 diluted PCR1, 1 U KAPA HIFI polymerase (KAPA Biosystems, KK2502), 0.3 mM dNTP mix, 0.4 µM each of TruSeq Universal Adapter and TruSeq Adapter with 6 bp index (Supplementary Table S4) in a total volume of 50 µL was performed to add Illumina sequencing adapters and 6 bp indexing primers using a program of 5 min at 95°C, followed by 5 cycles of 20 sec at 98°C, 15 sec at 60°C and 30 sec at 72°C, then 5 cycles of 20 sec at 98°C, 15 sec at 65°C and 30 sec at 72°C, and a 5 min final step at 72°C after the last cycle. The resultant 238 bp amplicon was purified using Axygen SPRI beads (AxyPrep FragmentSelect-I Kit, Axygen, MAGFRAG-I-50) at a PCR reaction to bead ratio of 1:1. Purified PCR products were sequenced for sgRNA frequency on a High Output Flow Cell Cartridge (Illumina, TG-160-2005) with the NextSeq500 system (Illumina, San Diego, California, USA) in a 75-bp single read configuration with a target average coverage of 100 reads per sgRNA at the in-house IRIC Genomics Platform. Context-dependent gene essentiality with the RANKS algorithm was scored as previously described (BERTOMEU *et al.* 2018). Gene Ontology term enrichment (THE GENE ONTOLOGY CONSORTIUM 2019) was calculated using custom scripts to determine FDR values and p-values (Fisher's exact test as implemented in R) (R CORE TEAM 2013). Mitochondrial genes were defined as belonging to the "mitochrondrion" Gene Ontology term.

CRISPR plasmids and sgRNA vector constructs. Lentiviral packaging vectors psPAX2 (#12260) and pCMV-VSV-G (#8454)(STEWART *et al.* 2003) and the Cas9/sgRNA lentiCRISPRv2GFP (#82416) (WALTER *et al.* 2017) vector were all obtained from Addgene. Lentiviral pLKO.1-puro vector carrying shRNA targeting CLPP mRNA (TRCN0000046858, TRCN0000046859, TRCN0000046860, TRCN0000046861, TRCN0000046862) and control vectors (MISSION PLKO.1-puro Empty Vector (SHC001), MISSION pLKO.1-puro Non-Mammalian shRNA Control Plasmid DNA (SHC002), Sigma) were obtained from the in-house IRIC High-Throughput Screening (HTS) platform. Human CLPP targeting sgRNAs and control sgRNRAs targeting AAVS1 and Azami-green were cloned into the LentiCRISPRv2GFP plasmid using sgRNA primers (Supplementary Table S4) and according to a protocol available at Addgene (https://www.addgene.org/crispr/zhang/). All plasmid, shRNA and sgRNA sequences are listed in Supplementary Table S5. Proper sgRNA

sequence insertion was confirmed by Sanger sequencing and transfection quality plasmid DNA was purified using a HiPure Plasmid filter (ThermoFisher Scientific, K210016).

Lentivirus production. Lentiviral particles carrying the CLPP targeting shRNAs were produced by transient calcium phosphate co-transfection of two helper plasmids (9 µg psPAX2 and 3 µg pCMV-VSV-G) along with the expression vector (7.5 µg pLKO-puro) into HEK293T cells at 70% confluence in 10-cm Petri dishes. After 6 h, medium was removed and replaced with DMEM 5% FBS (v/v) and after 48 h, lentivirus-bearing supernatants were collected and passed through a 0.45 µM filter. Lentiviral particles carrying CLPP or MIPEP targeting sgRNAs were produced by co-transfecting HEK293T cells with 28 µg psPAX2, 8 µg pCMV-VSV-G and 48 µg LentiCRISPRv2GFP vectors. After 6 h, media was changed to DMEM 10% FBS and sodium butyrate (Sigma, 303410) was added at a final concentration of 1 mM. The supernatant-containing particles were harvested 48 h after transfection and purified by 0.45 µm filtration. The virus-containing media were overlaid on a 6 mL sucrose cushion (20% w/v sucrose, 50 mM Tris-HCl, pH 7.4,100 mM NaCl, 0.5 mM ethylene diamine tetra acetic acid (EDTA)) at a 4:1 v/v ratio and concentrated by ultracentrifugation at 40,000 g for 120 minutes at 4^{o}C (Sorvall WX, SureSpin 630 Swinging Bucket). After centrifugation, the supernatants were removed, phosphate buffered saline (PBS) was added to the pelleted lentiviral particles to obtain a 100-fold virus concentration, and the tubes were placed on ice for 1 h with gentle agitation. Lentiviral particles were used immediately after preparation.

CLPP and MIPEP knockdown and knockout cell Lines. NALM-6 and RPE1-hTert cell lines down-regulated for CLPP expression were generated by lentiviral mediated transduction of shRNAs (NALM-6-shClpP-# and RPE1-hTert-shClpP-#). Lentiviral particles at a MOI of 0.5 were mixed with protamine sulfate (Sigma, P4020) at a concentration of 20 µg/mL in a volume of 1 mL and incubated for 30 min at room temperature (RT). Lentiviruses were subsequently added to 1 mL NALM-6 or RPE1-hTert cells at a concentration of 1,000,000 cells/mL. After incubation for 2 days, transduced cells were selected with puromycin (0.5 µg/mL for NALM-6; 3 µg/mL for RPE1-hTert) for 4 days and propagated until needed for experiments. Knockout populations of NALM-

6 cells were generated by the transduction of lentivirus vectors bearing a construct for the expression of the Cas9 nuclease and sgRNAs against CLPP or MIPEP (called NALM-6-sgRNA-CLPP# and NALM-6-sgRNA-MIPEP-#). NALM-6 cells at a concentration of 2,000,000 cells/mL in 5 mL were treated with 10 µg/mL protamine sulfate for 30 min at RT and concentrated lentiviral particles were added at a MOI of 0.7. Cells were incubated for 4 days and GFP positive cells were sorted on a BD FACSAria II (Franklin Lakes, New Jersey, USA) with FSC/SSC gating. Sorted cells were amplified and maintained in RPMI supplemented with 10% FBS (v/v) and 1% penicillin-streptomycin antibiotic (v/v) (Wisent, 325-043-EL) was added for 2 days to prevent bacterial contamination after cell sorting.

Protein extraction and immunoblot detection. NALM-6 cells were treated with 150 nM ONC212 or DMSO vehicle control for 72 h, lysed in RIPA buffer supplemented with 1 mM phenylmethylsulfonyl fluoride (PMFS) for 30 min on ice and lysates were clarified by centrifugation. Protein concentration was determined using a Pierce 660nm Protein Assay Kit (ThermoFisher Scientific, 22662). Yeast cells expressing the CLPP constructs or empty vector control were grown to OD_{600} = 1 and 5 mL of pelleted culture was lysed by incubation for 10 min at RT in 0.1 M NaOH and lysates were clarified by centrifugation. An equivalent protein amount for each sample was resolved on 10% or 15% SDS-PAGE (NALM-6) or by 15% SDS-PAGE (yeast) and transferred onto nitrocellulose membrane (GE Healthcare, GE10600001). Primary antibodies used for human CLPP detection and human MIPEP detection were mouse monoclonal anti-CLPP (Origene, TA502062) and rabbit polyclonal anti-MIPEP (GeneTex, GTX105574), respectively. Mouse monoclonal anti-PGK1 (Abcam, ab113687) or rabbit monoclonal anti-GAPDH (Cell Signaling Technology, 2118) were used as loading control for yeast or NALM-6 samples, respectively. Horseradish peroxidase conjugated goat anti-rabbit (Jackson Immuno Research Laboratory, 111-035-003) or goat anti-mouse (Jackson Immuno Research Laboratory, 115-035-146) were used as secondary antibodies. Blots were imaged using a ChemiDoc MP imaging system (BioRad) with Ultrascence Western Substrate (FroggaBio, CCH345-B100ML). Quantitation of protein species was performed using Image Lab software

version 6.0.1 (BioRad) and ratios expressed relative to the average of AAVS1 and Azami-green controls.

CLPP and ClpP in vitro enzymatic assays. Purified recombinant human CLPP or *E. coli* ClpP was resuspended at 10 µg/mL in 10 µL of assay buffer in presence of indicated compound concentrations and incubated for 20 min at 37°C in 384 well-plates in triplicate. Recombinant human CLPP was from Profoldin (Profoldin, USA , HMP100KE) and *E. coli* ClpP was produced and purified as described (LI *et al.* 2010; AHSAN 2014). Assay buffer was 50 mM HEPES pH 8, 10 mM MgCl2, 100 mM KCl, 0.02% Triton X-100, 1mM DTT and 5% glycerol (GRAVES *et al.* 2019). FITC-casein (20 µg/mL) or Ac-WLA-AMC (100 µM) were added and fluorescence intensity was recorded every 90 s for 60 min at 37°C and ($\lambda_{ex}/\lambda_{em}$) 485/528 nm or 350/460 nm for FITC-casein or Ac-WLA-AMC, respectively. For gel-based assays, 10 µg/mL recombinant purified human cLPP or *E. coli* bacterial ClpP was mixed with 100 ng/µL bovine α-casein in the presence of 100 µM ONC212 in assay buffer. The mixture was incubated at 30°C for 0 min, 60 min and 120 min, separated by 12% SDS-PAGE and stained with Coomassie Brilliant Blue.

Label-free quantitative proteome analysis. Systematic identification and quantification of the human and *S. aureus* proteomes was performed by LC-FAIMS-MS/MS analysis. NALM-6-shScrambled and NALM-6-shCLPP-46861 populations were treated with either 150 nM ONC212 or DMSO solvent control (final DMSO concentration of 0.1% v/v) for 24 h. Protein pellets were resuspended in 50 mM ammonium bicarbonate (NH_4HCO_3) with 10 mM TCEP [Tris(2-carboxyethyl)phosphine hydrochloride; Thermo Fisher Scientific] and incubated under agitation for 1 h at 37°C. Chloroacetamide (Sigma-Aldrich) was added for at 55 mM and incubated under agitation for 1 hr at 37°C. Samples were digested by 1 µg trypsin for 8 h at 37°C and, after drying, solubilized in 5% aqueous acetonitrile (ACN)-0.2% formic acid (FA). The samples were separated on a home-made reversed-phase column (150-µm i.d. x 20 cm) with a 56-min gradient from 10 to 30% ACN-0.2% FA and a 600-nL/min flow rate on an Easy-NLC 1000 connected to an Orbitrap Fusion equipped with FAIMS Pro™ and a nanoFlex ion source (Thermo Fisher Scientific, San Jose, CA)(PFAMMATTER *et al.* 2018). Each full MS spectrum acquired

at a resolution of 120,000 was followed by tandem-MS (MS^2) spectra on the most abundant multiply charged precursor ions using collision-induced dissociation (CID) at a collision energy of 30% and acquired in the ion trap. FAIMS CVs were stepped from -37V to -93V. The data were processed using PEAKS X (Bioinformatics Solutions, Waterloo, ON) and a human database. Mass tolerances on precursor and fragment ions were 10 ppm and 0.3 Da, respectively. Variable selected posttranslational modifications were carbamidomethyl (C), oxidation (M), deamidation (NQ), phosphorylation (STY) and acetylation (N-ter). The data were visualized with Scaffold 4.3.0 (protein threshold 99%, with at least 2 peptides identified and a false-discovery rate (FDR) of 1% for peptides).

Stationary phase *S. aureus* (ATCC29213) cells were treated with 30 µM ONC212 or DMSO solvent control for 10 min, 40 min and 24 h at 37°C in biological replicate. Cell pellets were resuspended 8 M urea, 50 mM Tris pH8.0 and lysed using a Freezer Mill (Spex®SamplePrep) and cleared by centrifugation. 200 µg of total protein was reconstituted at 1 µg/µL in 100 mM $(NH_4)HCO_3$, 5 mM TCEP and incubated for 1 h at 37°C with agitation at 400 rpm. Chloroacetamide was added to 55 mM, samples were incubated at 37°C and 400 rpm for 1 h, and the digested by 10 µg trypsin overnight at 37°C and 400 rpm. Desalted samples were reconstituted at 1 µg/µL in 4% FA and loaded on a home-made C18 column (3 µm C18 Jupiter Phenomenex, 150 µm x 25 cm). Peptides were separated using a linear gradient of 5–30% ACN (0.2% FA) for 220 min at a flow rate of 600 nL/min. A FAIMS PRO™was interfaced to a nanospray Flex ion source coupled to an Orbitrap Fusion (Thermo Fisher Scientific) as described previously (PFAMMATTER *et al.* 2018). The inner and outer electrode temperature were both set to 100°C and the dispersion voltage (DV) was set at −5000 V. Each sample was injected three times using the three-stepped CV combination (CV -37 V/-44 V/-51 V, CV -58 V/-65 V, and CV -72 V/-79 V/-86 V/-93 V). Spray voltage was set to 2,800 V. Full MS (range from m/z 350 to m/z 890) in the Orbitrap were acquired at 240,000 resolution followed by a top speed MS^2 acquisition of 3 s acquired in the linear ion trap. Maximal injection time for full MS was 50 ms with an AGC of 5e5. Maximal injection time for MS2 was 35 ms with an AGC of 2e4. For MS2 triggering, only charge states 2–6 were selected at a collision energy of 30% and an isolation window width of 1.0 Th. Data were analyzed as above for NALM-6 cells but with a *S. aureus*

ATCC29213 custom database constructed from the draft *S. aureus* ATCC29213 genome sequence (SONI *et al.* 2015). This custom database improved protein detection sensitivity and proteome coverage due to inherent genetic variability between different *S. aureus* strains. The maximum number of missed cleavages for trypsin was set to 3 and phosphorylation modifications (STY) were not included. Deamidation (NQ) and oxidation (M) were set as variable modifications and carbamidomethylation (C) set with a maximum of three modifications per peptide.

To identify non-tryptic peptides, peaks were extracted to mascot generic format (mgf) using the ProteoWizard Toolkit 3.0.6839 (CHAMBERS *et al.* 2012) and spectra compared to theoretical spectra of all possible peptides between 8 and 20 residues long using in-house code, applying a precursor and fragment tolerance of 0.3 Da and a minimum of 6 matched fragment ion peaks per peptide identification. Peptide modifications were not considered. Non-tryptic peptide fold-changes were estimated only for proteins with at least two unique peptides identified. Position-specific residue preferences around non-tryptic cleavage sites were restricted to peptides with at least 8 matched fragment ion peaks or supported by two or more spectra.

In order to compare *S. aureus* proteomics results to a previously published dataset (CONLON *et al.* 2013), and to map Gene Ontology annotations and gene essentiality information from other analyses (CHAUDHURI *et al.* 2009), identification of the closest homologs across divergent strains of *S. aureus* was required. For each of the three strains (COL, C0673 and Mu50), all protein sequences from UniProt (THE UNIPROT CONSORTIUM 2017) were obtained and SSEARCH version 36.3.5c (PEARSON 2000) was used to identify all alignments with an E-value of less than 0.01. Proteins with the lowest E-value were considered as the closest homolog.

High content image analysis of mitochondrial function. NALM-6 cells were treated for 72 h with two-fold serial dilutions of ONC201 (0.3-10 µM), ONC212 (0.03-1 µM), the ONC201 (TIC10)-inactive isomer (0.3-10 µM) or DMSO solvent control in RPMI1640 + 10%FBS. NALM-6 cells treated for 16 h with doxorubicin (2 µM; MedChemExpress, HY-15142) were used as a positive control for mitochondrial damage and production of reactive oxygen species (ROS).

Cells were pelleted by centrifugation (5 min at 300 x g) and washed with 100 µL PBS at 37°C. Combinations of cell permeable dyes were added in imaging medium (RPMI 1640 without phenol red (Wisent, 350-046-CL) + 10% FBS v/v) at 37°C. For membrane potential, indicator dyes for mitochondrial mass (MitoSpy GreenFM, Biolegend, #424805) and membrane potential (MitoSpyRed CMXRos, Biolegend, #424801) were used at a final concentration of 100 nM. For mitochondrial reactive oxygen species (ROS), indicator dyes for ROS (MitoSox Red, ThermoFisher Scientific, #M36008) and DNA (propidium iodide (PI); Biotium, #40017) were used at 5 µM and 1.5 µM, respectively. Cells were incubated for 30 min with the dye combinations while protected from light, then pelleted and washed twice, resuspended in imaging medium and transferred to 96-well imaging plates (Greiner Screenstar, #655866). Plates were imaged on an OPERA high-throughput confocal spinning disk microscopy platform (PerkinElmer) within 30-45 minutes of plating. Imaging was performed using a 60x water objective and 2*2 pixel binning, which corresponded to 148.18um FOVs with a 220nm pixel size resolution. The MitoSpy GreenFM/MitoSpyRed, and MitoSox/PI dyes pairs were sequentially excited respectively using 488nm and 561nm lasers at maximal power for short durations (40-200ms), and the emitted fluorescence signals were collected using 525nm±35nm and 600±40nm bandpass filters. All experiments were performed in triplicate.

Analysis was performed with Acapella software. Individual cells were masked based on pixel intensity using Acapella masking routines and visually confirmed on sample images for all conditions. Cells cropped at the border of fields of views (FOVs) and cell showing no MitoSpy GreenFM staining or strong PI staining were eliminated from further analysis. Unseparated cell clusters and other detection artefacts were filtered out using large and small cell area thresholds and cell roundness-based morphological selection. Acapella spot detection was performed on the MitoSpy GreenFM signal to localize mitochondria and restrict further calculations to mitochondrial image regions. Membrane potential was assessed by normalizing MitoSpyRed fluorescence intensity to mitochondrial mass (MitoSpy GreenFM intensity) in each individual cell, and averaging over cell populations within each well and across three in-plate replicates. Mitochondrial ROS levels were determined from the cell-averaged MitoSox

fluorescence intensity within each well across three in-plate replicates. Residual weak PI staining bleeding through the MitoSox channel made only a minor contribution.

Yeast strains and culture. Yeast strains used in this study were isogenic with *Saccharomyces cerevisiae* S288C (BY4741) and are listed in Supplementary Table S6. Yeast transformants bearing human CLPP or bacterial ClpP expression plasmids were selected on synthetic complete (SC) medium without histidine (-His) and 2% w/v glucose. For induction, glucose was replaced by 1% w/v raffinose (Raf) and 1% w/v galactose (Gal). Yeast ClpP expression vectors were constructed with codon- and GC content-optimized synthetic genes from commercial providers (Bio Basic, Markham, ON, Canada; IDT, Coralville, USA). Amino acids 1 to 195 from *S. aureus* ClpP (UniProt P63786) and amino acids 1 to 277 or 57 to 277 from *Homo sapiens* CLPP (UniProt Q16740) were used to construct full length *S. aureus* ClpP (MT4638), full length propeptide-containing human CLPP (MT4639) and processed mature human CLPP (MT4641), respectively. Mutations to create a proCLPP mutant with a scrambled MIPEP recognition site within the octapeptide residues of the MPP/MIPEP R-10 cleavage motif (GAKH *et al.* 2002) were introduced by site directed mutagenesis (MT4640). Gene coding regions were inserted between the *GAL1* promoter and *GYP7* terminator in a modified pRS313 vector (MT4637) that was created by PCR of pRS313 (ATCC 77142) with primers YAC0638 and YAC0489, followed by insertion of PCR fragments of the *GYP7* terminator (YAC0639, YAC0479), dual *GAL1*/*GAL10* promoter (YAC0478, YAC0624), *FUM1* terminator (YAC0625, YAC0484), *GAL7* promoter (YAC0485, YAC0507) and *CYC7* terminator (YAC0487, YAC0488) fragments using isothermal assembly (GIBSON *et al.* 2009). All promoters and terminators were amplified from genomic DNA of strain BY4742 (ATCC 4011119). MT4637 was opened by PCR with the primers YAC0499 and YAC0502 and genes encoding *S. aureus* ClpP (YAC0650, YAC0651), human proCLPP (YAC0690, YAC0691), human proCLPP mutant (YAC0690, YAC0691) and human CLPP (YAC0690, YAC0692) were inserted between the *GAL1* promoter and *GYP7* terminator by isothermal assembly to yielded plasmids MT4638, MT4639, MT4640 and MT4641, respectively. Yeast were transformed by the standard LiAc/SS carrier DNA/PEG method (GIETZ AND SCHIESTL 2007). Oligonucleotide sequences for all constructions are provided in Supplementary Table S4 and complete DNA sequences of

constructs are provided in Supplementary Table S5. For growth rate determination, strains expressing human CLPP and bacterial ClpP constructs were cultured in SC-His+Raf/Gal medium in 96-well flat bottom microtiter plates. Saturated cells were diluted to OD_{600} = 0.03 and grown in presence of increasing concentrations of compounds at 30°C with continuous shaking. Absorbance readings at 595 nm were taken at 15 min intervals in an automated UV-VIS plate shaker-reader (Tecan Sunrise). Apparent MICs were calculated as relative cell growth in wells of compounds versus medium-only controls. Data from at least two independent biological experiments each with duplicates were plotted using Prism software (GraphPad.com).

Bacterial culture and MIC determination. Minimal inhibitory concentrations of ONC201, ONC212 or ADEP1 for the various bacterial species were determined according to the CLSI (2015) guidelines (CLSI 2015). Bacterial strains used in this study are listed in Supplementary Table S7. Culture densities were determined at OD_{600} using a Spectramax 384 Plus after shaking plates for 5 min. *B. subtilis*, *S. aureus*, *E. faecium*, *K. pneumonia*, *A. baumannii*, *P. aeruginosa* and *E. aerogenes* were cultured in cation-adjusted Mueller-Hinton broth (CAMHB). Overnight cultures were suspended in 0.85% saline solution to OD_{625} = 1, diluted 1/200 in 100µL fresh medium with indicated drug amounts in transparent 96-flat bottom plates and incubated for 24 h at 37°C without shaking prior to density determination. *N. gonorrhoeae* was cultured in gonococcal base agar solid medium (GCB, Difco) with 1% Kellogg's supplements. After incubation for 18–20 h at 37°C under 5% CO_2, colonies were sub-cultured onto GCB plates. After 20-24 h, colonies were resuspended in liquid GCB media at OD_{625} = 0.1 and 100 µL of a 1/200 dilution was added to a transparent 96-round bottom plate that contained appropriate aliquots of each drug or solvent control. Plates were incubated at 37°C at 5% CO_2 and 90% humidity with agitation at 220 rpm for 20 h prior to density determination. *M. smegmatis* was cultured in Middlebrook 7H9 Broth for 48 h at 37°C then resuspended in fresh medium at OD_{625} = 0.1, diluted 1/200 in 100 µL fresh medium with indicated drug amounts in transparent 96-flat bottom plates, and incubated for 48 h at 37°C without shaking prior to density determination. *M. tuberculosis* H37Ra was cultured in Middlebrook 7H9 Broth. Cultures were started by diluting 1 mL of frozen *M. tuberculosis* stock in 19 mL of fresh media and incubating at 37°C at

225 rpm for four or five days until OD_{600} reached between 0.4 and 0.8. Cultures were centrifuged at 70 x g for 5 min at RT to pellet any aggregated cells then 100 µL of the supernatant was added to each well of a transparent 96-flat bottom plate with indicated drug amounts. Plates were sealed to prevent evaporation and incubated at 37°C for 7 days without agitation. 20 µL of resazurin dye (filter sterilized, 0.15 mg/mL) was then added to each well and incubated for an additional 24 h at 37°C. Growth was assessed by the conversion of resazurin into resorufin product by red fluorescence.

Disk diffusion assays. *S. aureus* (ATCC29213) and *E. coli* were grown overnight in LB media at 37°C and 225rpm. 100 µL of culture was plated on LB agar plates and disks were placed on the plate. Yeast strains were grown in SC-His+Raf for 12 h at 30°C and 225rpm. 100µL of culture was plated on SC-His+Raf/Gal agar plates and disks were placed on the plate. Indicated doses of ONC201, ONC212 or DMSO in 10 µL were spotted on disks. Bacterial plates incubated at 37°C for 24 h and yeast plates were incubated at 30°C for 48 h prior to imaging with a DSLR camera (Canon EOS T3i).

Antibiotic synergy and biofilm assays. *S. aureus* (ATCC29213) was cultivated overnight in LB at 37°C and 225 rpm. Overnight cultures were diluted 1/200 in fresh medium. Indicated amounts of each drug or DMSO control were added to a transparent 96-flat bottom plates by acoustic transfer (Labcyte Echo 555) and 100 µL of bacterial solution added to each well. Plates were sealed to avoid evaporation, incubated for 24 h at 37°C and 190 rpm, and culture density determined at OD_{600} using a microplate reader (Tecan Infinite M1000 Pro).

S. aureus biofilms were grown as described (CONLON *et al.* 2013). Overnight *S. aureus* (ATCC29213) culture was diluted 1:20 in brain heat infusion (BHI) broth and dispensed at 100 µL/well in a polystyrene 96 well plate. Plates were incubated for 48 h at 37^{o} C without shaking, after which medium was aspirated and plates were gently washed twice with 100 µL/well PBS. Antibiotics were added at indicated concentrations in 150 µL fresh BHI per well and plates incubated for 72 h at 37^{o}C. Medium was aspirated, wells washed twice with 100 µL/well PBS then biofilm cells were dislodged by sonication in 100 µL/well PBS for 5 min in a sonicating

water bath at RT. Five µL of cell suspension was added to 145 µL of LB and growth was monitored at 5 min intervals for 16 h at OD_{595} at 37°C and 300 rpm using an absorbance plate reader (Sunrise, Tecan). The method for estimation of the number of surviving persister cells was adapted from (HAZAN *et al.* 2012). The time to reach A_{595} = 0.15 was converted to CFU using a standard curve of *S. aureus* log CFU versus time to reach A_{595} = 0.15. A standard curve was constructed by diluting 5 µL *S. aureus* overnight culture in 140 µL LB supplemented with 5 µL PBS. Serial ten-fold dilutions were made over 8 orders of magnitude in LB + 5 µL PBS. The time to reach A_{595} 0.15 for each dilution was measured as above and CFU determined by plating 7 µL of cell dilution on a LB agar plate and counting colonies after incubation overnight at 37° C. Cell numbers above or below ~600 cells/mL were determined by interpolation or extrapolation of the standard curve, respectively.

In silico docking and structural superposition. Ligand docking was performed using Autodock VINA (TROTT AND OLSON 2010) using default parameters and X-ray crystal structures of CLPP in complex with an ADEP analog (PDB code 6BBA) and CLPP in complex with the non-ADEP small molecule activator D9 (PDB code 6H23) as template structures (STAHL *et al.* 2018; WONG *et al.* 2018). As bacterial ClpP template structures, the ClpP-ADEP crystal structures of *E. coli* (PDB 3mt6)(LI *et al.* 2010), *B. subtilis* (PDB 3kti)(LEE *et al.* 2010) and *S. aureus* (PDB 5vz2) were used. The docking site was limited to two adjacent ClpP monomer units (global docking mode) or to the ADEP binding pocket (local docking mode). Template structures were prepared for docking by adding hydrogen atoms, structures were energy minimized and water and ligands were removed. Residue Ala 118 of template structure 6H23 was replaced by Tyr to represent the human wild-type CLPP structure. The entire workflow, including ligand and receptor structure preparation and docking setup, was implemented in the YASARA Structure molecular modeling program (www.yasara.com) (KRIEGER *et al.* 2002). The docked conformer with the best score was used. Structural superpositions of ClpP-ADEP structures or the ClpP-D9 structure with the CLPP-ONC201 structure (PDB code 6DL7) (ISHIZAWA *et al.* 2019) were generated with PyMOL Version 2.3 (Schrödinger, LLC).

Supplementary Discussion associated with Supplementary Figure 5

Molecular interactions of ONC201 with human CLPP have been described previously based on the X-ray structure of ONC201 in complex with human CLPP (PDB code 6DL7) (ISHIZAWA *et al.* 2019; WONG AND HOURY 2019). ONC201 occupies the same groove as ADEPs between two adjacent CLPP monomers (ISHIZAWA *et al.* 2019). Even though ONC201 is substantially smaller than ADEP analogs, it recapitulates many ADEP-CLPP interactions (PDB code 6BBA)(WONG *et al.* 2018). Thus, the benzyl moiety of ONC201 inserts in the same hydrophobic pocket as the derivatized benzoyl moieties of ADEP analogs. This pocket is comprised of Tyr118, Val148, Leu170 of one CLPP monomer and Leu104, Thr135 and Tyr138 of the adjacent CLPP monomer. The phenylmethyl moiety of ONC201 extends into the same binding groove as the aliphatic tails of ADEPs, formed by the C-atoms of CLPP residues Leu104 and Ser108 in one monomer and Leu79, Glu82 and Ile84 of the adjacent monomer. The tricyclic imipridone core extends to the same position as the beta-methylproline moiety of the ADEP core and interacts with residues His116, Trp146, Leu245 and Tyr118 of CLPP.

Structural superimposition and molecular docking of ONC201 and ONC212 in ClpP-ADEP structures from several bacterial species (i.e., *E. coli* (ecClpP; PDB 3MT6), *B. subtilis* (bsClpP; PDB 3KTI) and *S. aureus* (saClpP; PDB 5VZ2)) indicates that the binding pockets in bacterial ClpP could also accommodate the imipridones in a similar orientation while retaining many interactions observed with human CLPP. Most of the residues lining the hydrophobic pocket of CLPP are conserved in ClpP from different bacterial species. Only residues at equivalent positions to Val148 and Tyr138 in human CLPP differ in bacterial ClpP orthologs: Val148 is replaced by various other non-aromatic hydrophobic residues, whereas Tyr138 is substituted by Phe in ecClpP and bsClpP, and His in saClpP. The phenylmethyl binding groove is also similar: Glu82 of human CLPP is substituted by Asp in bsClpP and saClpP, while Ser108 is replaced by Ala in all bacterial forms. Larger differences occur in the residues supporting the tricyclic imipridone core: while Tyr118 is invariant between human CLPP and bacterial ClpP, His116 is Tyr in ecClpP and saClpP, and Ser in bsClpP. This Ser substitution might explain the lower activity of ONC212 against bsClpP versus saClpP. The Ser of bsClpP does not contribute to favorable interactions

with the imidazole ring of the tricyclic imipridone core, unlike the corresponding Tyr residue in saClpP. The largest difference between human CLPP and bacterial ClpP orthologs is human residue Trp146, which is substituted by substantially smaller Ile or Val residues in bacteria. This divergent feature might be used to design imipridone analogs that are more highly selective for bacterial ClpP versus human CLPP.

Comparison of the human CLPP co-structures with D9 (PDB 6H23) (STAHL *et al.* 2018) and ONC201 (ISHIZAWA *et al.* 2019) suggest that the methylbenzyl of ONC201 (or trifluoromethylbenzyl moiety of ONC212) might be substituted with a larger benzodioxiole moiety that extends further into the binding groove on CLPP. To date, SAR on the imipridone scaffold has been mainly limited to smaller substituents around this moiety (WAGNER *et al.* 2017; GRAVES *et al.* 2019). Similarly, existing SAR on substituents around the benzyl moiety of ADEPs or the benzylmoiety of imipridone and TR series compounds suggest that small mono or di-substituents (e.g., halogen or nitrile groups) might also improve binding energy in this pocket (BROTZ-OESTERHELT *et al.* 2005; GRAVES *et al.* 2019). These modifications might benefit interactions with human CLPP and bacterial ClpP to a similar extent. Based on structural super-positioning or molecular docking of the imipridones in *Mycobacterium tuberculosis* ClpP2 (mtClpP2) (PDB 4U09)(SCHMITZ *et al.* 2014) it is not immediately clear why ONC201 is moderately active against this species, whereas ONC212 is not active. The pocket that accommodates the methylbenzyl moiety of ONC201 should also be able to accommodate the slightly larger trifluoromethylbenzyl moiety of ONC212. Like bsClpP, mtClpP2 has a relatively small amino acid residue (Thr) at the equivalent position to His116 in human CLPP. The lack of favorable interactions with the imipridone tricyclic core might help explain the relatively weak activity of the imipridones against *Mycobacterium* spp. Other cellular attributes undoubtedly contribute to the resistance of mycobacteria to the imipridones, including the cell wall barrier and the unusual activation mechanism of the atypical mtClpP1-P2 protease system. Intriguingly, ADEPs appear to kill mycobacteria by inhibiting rather than activating ClpP function (FAMULLA *et al.* 2016), a possibility we cannot rule out based on our cell-based activity assays alone. With respect other possible pathogen targets, imipridone analogs active against *Plasmodium*

falciparum ClpP (pfClpP) (PDB 2F6I)(EL BAKKOURI *et al.* 2010) or other protozoan ClpP orthologs would likely require more drastic modifications due to the less conserved methylbenzyl binding groove in these species, which is substantial smaller due to the presence of Phe residues at the equivalent positions of Arg78 and Leu79 in human CLPP. In addition, the tricyclic imipridone core would not be tightly engaged in protazoan ClpP due to the presence of Lys and Ile residues at equivalent positions of His 116 and Trp147 in human CLPP, respectively.

Supplementary References

Ahsan, B., 2014 Understanding the activation of bacterial protease ClpP by acyldepsipeptide antibiotic, pp. 75 in *Biochemistry and Biomedical Sciences*. McMaster University, Hamilton, Ontario.

Bertomeu, T., J. Coulombe-Huntington, A. Chatr-Aryamontri, K. G. Bourdages, E. Coyaud *et al.*, 2018 A High-Resolution Genome-Wide CRISPR/Cas9 Viability Screen Reveals Structural Features and Contextual Diversity of the Human Cell-Essential Proteome. Mol Cell Biol 38.

Brachmann, C. B., A. Davies, G. J. Cost, E. Caputo, J. Li *et al.*, 1998 Designer deletion strains derived from Saccharomyces cerevisiae S288C: a useful set of strains and plasmids for PCR-mediated gene disruption and other applications. Yeast 14**:** 115-132.

Brotz-Oesterhelt, H., D. Beyer, H. P. Kroll, R. Endermann, C. Ladel *et al.*, 2005 Dysregulation of bacterial proteolytic machinery by a new class of antibiotics. Nat Med 11**:** 1082-1087.

Chambers, M. C., B. Maclean, R. Burke, D. Amodei, D. L. Ruderman *et al.*, 2012 A cross-platform toolkit for mass spectrometry and proteomics. Nat Biotechnol 30**:** 918-920.

Chaudhuri, R. R., A. G. Allen, P. J. Owen, G. Shalom, K. Stone *et al.*, 2009 Comprehensive identification of essential Staphylococcus aureus genes using Transposon-Mediated Differential Hybridisation (TMDH). BMC Genomics 10**:** 291.

CLSI (Editor), 2015 *Methods for Dilution Antimicrobial Susceptibility Tests for Bacteria That Grow Aerobically; Approved Standard—Tenth Edition*. Clinical and Laboratory Standards Institute, Wayne, PA.

Conlon, B. P., E. S. Nakayasu, L. E. Fleck, M. D. LaFleur, V. M. Isabella *et al.*, 2013 Activated ClpP

kills persisters and eradicates a chronic biofilm infection. Nature 503**:** 365-370.

Dasari, S., and R. Kolling, 2016 Role of mitochondrial processing peptidase and AAA proteases in processing of the yeast acetohydroxyacid synthase precursor. FEBS Open Bio 6**:** 765-773.

Doench, J. G., N. Fusi, M. Sullender, M. Hegde, E. W. Vaimberg *et al.*, 2016 Optimized sgRNA design to maximize activity and minimize off-target effects of CRISPR-Cas9. Nat Biotechnol 34**:** 184-191.

El Bakkouri, M., A. Pow, A. Mulichak, K. L. Cheung, J. D. Artz *et al.*, 2010 The Clp chaperones and proteases of the human malaria parasite Plasmodium falciparum. J Mol Biol 404**:** 456-477.

Famulla, K., P. Sass, I. Malik, T. Akopian, O. Kandror *et al.*, 2016 Acyldepsipeptide antibiotics kill mycobacteria by preventing the physiological functions of the ClpP1P2 protease. Mol Microbiol 101**:** 194-209.

Gakh, O., P. Cavadini and G. Isaya, 2002 Mitochondrial processing peptidases. Biochim Biophys Acta 1592**:** 63-77.

Gibson, D. G., L. Young, R. Y. Chuang, J. C. Venter, C. A. Hutchison, 3rd *et al.*, 2009 Enzymatic assembly of DNA molecules up to several hundred kilobases. Nat Methods 6**:** 343-345.

Gietz, R. D., and R. H. Schiestl, 2007 Large-scale high-efficiency yeast transformation using the LiAc/SS carrier DNA/PEG method. Nat Protoc 2**:** 38-41.

Graves, P. R., L. J. Aponte-Collazo, E. M. J. Fennell, A. C. Graves, A. E. Hale *et al.*, 2019 Mitochondrial Protease ClpP is a Target for the Anticancer Compounds ONC201 and Related Analogues. ACS Chem Biol 14**:** 1020-1029.

Hazan, R., Y. A. Que, D. Maura and L. G. Rahme, 2012 A method for high throughput determination of viable bacteria cell counts in 96-well plates. BMC Microbiol 12**:** 259.

Ishizawa, J., S. F. Zarabi, R. E. Davis, O. Halgas, T. Nii *et al.*, 2019 Mitochondrial ClpP-Mediated Proteolysis Induces Selective Cancer Cell Lethality. Cancer Cell 35**:** 721-737 e729.

King, A. M., S. A. Reid-Yu, W. Wang, D. T. King, G. De Pascale *et al.*, 2014 Aspergillomarasmine A overcomes metallo-beta-lactamase antibiotic resistance. Nature 510**:** 503-506.

Krieger, E., G. Koraimann and G. Vriend, 2002 Increasing the precision of comparative models with YASARA NOVA--a self-parameterizing force field. Proteins 47**:** 393-402.

Lee, B. G., E. Y. Park, K. E. Lee, H. Jeon, K. H. Sung *et al.*, 2010 Structures of ClpP in complex with acyldepsipeptide antibiotics reveal its activation mechanism. Nat Struct Mol Biol 17**:** 471-478.

Li, D. H., Y. S. Chung, M. Gloyd, E. Joseph, R. Ghirlando *et al.*, 2010 Acyldepsipeptide antibiotics induce the formation of a structured axial channel in ClpP: A model for the ClpX/ClpA-bound state of ClpP. Chem Biol 17**:** 959-969.

Meyers, R. M., J. G. Bryan, J. M. McFarland, B. A. Weir, A. E. Sizemore *et al.*, 2017 Computational correction of copy number effect improves specificity of CRISPR-Cas9 essentiality screens in cancer cells. Nat Genet 49**:** 1779-1784.

Msadek, T., V. Dartois, F. Kunst, M. L. Herbaud, F. Denizot *et al.*, 1998 ClpP of Bacillus subtilis is required for competence development, motility, degradative enzyme synthesis, growth at high temperature and sporulation. Mol Microbiol 27**:** 899-914.

Pearson, W. R., 2000 Flexible sequence similarity searching with the FASTA3 program package. Methods Mol Biol 132**:** 185-219.

Pfammatter, S., E. Bonneil, F. P. McManus, S. Prasad, D. J. Bailey *et al.*, 2018 A Novel Differential Ion Mobility Device Expands the Depth of Proteome Coverage and the Sensitivity of Multiplex Proteomic Measurements. Mol Cell Proteomics 17**:** 2051-2067.

Piotrowski, J. S., S. C. Li, R. Deshpande, S. W. Simpkins, J. Nelson *et al.*, 2017 Functional annotation of chemical libraries across diverse biological processes. Nat Chem Biol 13**:** 982-993.

R Core Team, 2013 R: A language and environment for statistical computing. R Foundation for Statistical Computing, Vienna, Austria. URL http://www.R-project.org/.

Schmitz, K. R., D. W. Carney, J. K. Sello and R. T. Sauer, 2014 Crystal structure of Mycobacterium tuberculosis ClpP1P2 suggests a model for peptidase activation by AAA+ partner binding and substrate delivery. Proc Natl Acad Sci U S A 111**:** E4587-4595.

Soni, I., H. Chakrapani and S. Chopra, 2015 Draft Genome Sequence of Methicillin-Sensitive Staphylococcus aureus ATCC 29213. Genome Announc 3.

Stahl, M., V. S. Korotkov, D. Balogh, L. M. Kick, M. Gersch *et al.*, 2018 Selective Activation of Human Caseinolytic Protease P (ClpP). Angew Chem Int Ed Engl 57**:** 14602-14607.

Stewart, S. A., D. M. Dykxhoorn, D. Palliser, H. Mizuno, E. Y. Yu *et al.*, 2003 Lentivirus-delivered stable gene silencing by RNAi in primary cells. RNA 9**:** 493-501.

The Gene Ontology Consortium, 2019 The Gene Ontology Resource: 20 years and still GOing strong. Nucleic Acids Res 47**:** D330-D338.

The UniProt Consortium, 2017 UniProt: the universal protein knowledgebase. Nucleic Acids Res 45**:** D158-D169.

Trott, O., and A. J. Olson, 2010 AutoDock Vina: improving the speed and accuracy of docking with a new scoring function, efficient optimization, and multithreading. J Comput Chem 31**:** 455-461.

Wagner, J., C. L. Kline, M. D. Ralff, A. Lev, A. Lulla *et al.*, 2017 Preclinical evaluation of the imipridone family, analogs of clinical stage anti-cancer small molecule ONC201, reveals potent anti-cancer effects of ONC212. Cell Cycle 16**:** 1790-1799.

Walter, D. M., O. S. Venancio, E. L. Buza, J. W. Tobias, C. Deshpande *et al.*, 2017 Systematic In Vivo Inactivation of Chromatin-Regulating Enzymes Identifies Setd2 as a Potent Tumor Suppressor in Lung Adenocarcinoma. Cancer Res 77**:** 1719-1729.

Wong, K. S., and W. A. Houry, 2019 Chemical Modulation of Human Mitochondrial ClpP: Potential Application in Cancer Therapeutics. ACS Chem Biol 14**:** 2349-2360.

Wong, K. S., M. F. Mabanglo, T. V. Seraphim, A. Mollica, Y. Q. Mao *et al.*, 2018 Acyldepsipeptide Analogs Dysregulate Human Mitochondrial ClpP Protease Activity and Cause Apoptotic Cell Death. Cell Chem Biol 25**:** 1017-1030 e1019.

Supplementary Tables

Supplementary Table S4. Primer sequences.

primer	sequence
sgRNA CLPP-1 Forward	5’-CACCGGATCATGATACGGGAGTTG-3’
sgRNA CLPP-1 Reverse	5’-AAACCAACTCCCGTATCATGATCC-3’
sgRNA CLPP-2 Forward	5’-CACCGCGCCTATGACATCTACTCG-3’
sgRNA CLPP-2 Reverse	5’-AAACCGAGTAGATGTCATAGGCGC-3’
sgRNA CLPP-3 Forward	5’-CACCGAGCGAGTGGCGCATGCCTG-3’
sgRNA CLPP-3 Reverse	5’-AAACCAGGCATGCGCCACTCGCTC-3’
sgRNA MIPEP-1 Forward	5’-CACCGCCAGCATTCAGAGAAGCTG-3’
sgRNA MIPEP-1 Reverse	5’-AAACCAGCTTCTCTGAATGCTGGC-3’
sgRNA MIPEP-2 Forward	5’-CACCGTAGCACCATACCCCACGAGG-3’
sgRNA MIPEP-2 Reverse	5’-AAACCCTCGTGGGGTATGGTGCTAC-3’
sgRNA MIPEP-3 Forward	5’-CACCGCAGCACCAGCTGGTCTCCCG-3’
sgRNA MIPEP-3 Reverse	5’-AAACCAGCACCAGCTGGTCTCCCGC-3’
sgRNA AAVS1 Forward	5’-CACCGGGGCCACTAGGGACAGGAT-3’
sgRNA AAVS1 Reverse	5’-AAACATCCTGTCCCTAGTGGCCCC-3’
sgRNA Azami-green Forward	5’-CACCGGCCACAACTTCGTGATCGA-3’
sgRNA Azami-green Reverse	5’-AAACTCGATCACGAAGTTGTGGCC-3’
Outer Primer-1	5’-AGCGCTAGCTAATGCCAACTT-3’
Outer Primer-2	5’-GCCGGCTCGAGTGTACAAAA-3’
TruSeq Universal Adapter	5’-AATGATACGGCGACCACCGAGATCTACACTCTTTCCCTACACGACGCTCTTCCGATCTCTTGTGGAAAGGACGAAACA-3’
TruSeq Adapter with 6bp index	5’-CAAGCAGAAGACGGCATACGAGAT(NNNNNN)GTGACTGGAGTTCAGACGTGTGC TCTTCCGATCCACCGACTCGGTGCCACTTTT-3’

YAC0478	5'-TTCTATTTACCAGGGTTTTTTCTCCTTGACGTTAAAGTATAGAGG-3'
YAC0479	5'-GAGAAAAAACCCTGGTAAATAGAAACGGAACTTTACATATTGAATACCG-3'
YAC0484	5'-TAAGCTGGCAAAGGACCATTGCTGAATCACAAATTCTCTC-3'
YAC0485	5'-CAGCAATGGTCCTTTGCCAGCTTACTATCCTTCTTGAAAATATGC-3'
YAC0487	5'-ATTCCCTCAAAAGCTATGTCGTCGGAGGAGATATTTATTACTTTTATTATTCTAG-3'
YAC0488	5'-AAAATGTATTAATAAATAAAAGAACTTAAATATAGACTTTTTATTCGC-3'
YAC0489	5'-TTCTTTTATTTATTAATACATTTTCCAGGAACCGTAAAAAGGCCG-3'
YAC0499	5'-GGGTTTTTTCTCCTTGACGTTAAAGTATAGAGG-3'
YAC0502	5'-TGGTAAATAGAAACGGAACTTTACATATTGAATACC-3'
YAC0507	5'-TTTTGAGGGAATATTCAACTGTTTTTTTTTATCATGTTG-3'
YAC0624	5'-TCTTACTTTTTTTTTGGATGGACGCAAAGAAG-3'
YAC0625	5’-CGTCCATCCAAAAAAAAAGTAAGAATTTTTGAAAACG-3’
YAC0638	5’-CGAAACGGAAAAACTGAAGAAAAAGCATCTGTGCGGTATTTCACACC-3’
YAC0639	5’-TTTTTCTTCAGTTTTTCCGTTTCGGGCG-3’
YAC0650	5’-GTAAAGTTCCGTTTCTATTTACCATTATTTTGTTTCAGGTACCATCACTTCATCAATTAGG-3’
YAC0651	5'-TTTAACGTCAAGGAGAAAAAACCCATGAATTTAATTCCTACAGTTATTGAAACAACAAACCG-3'
YAC0690	5'-GTAAAGTTCCGTTTCTATTTACCATCAGGTGCTAGCTGGAACAGG-3'
YAC0691	5'-TTTAACGTCAAGGAGAAAAAACCCATGTGGCCGGGAATACTTGTCG-3'
YAC0692	5’-TTTAACGTCAAGGAGAAAAAACCCATGCCTTTAATCCCAATAGTGGTGGAACAAACG-3'

Supplementary Table S5. Plasmids and DNA sequences.

plasmid	insert	base vector	source
psPAX2	none	none	Laboratory of Didier Trono (Addgene: 12260)
pCMV-VSV-G	none	none	STEWART *et al.* 2003 (Addgene: 8454)
MISSION PLKO.1-puro Empty vector control	none	none	SHC001 (Sigma)
MISSION pLKO.1-puro Non-Mammalian shRNA Control Plasmid DNA	none	none	SHC002 (Sigma)
LentiCRISPRv2GFP	none	none	WALTER *et al.* 2017 (Addgene: 82416)
MT4637	none	pRS313	ATCC77142 (ATCC)
MT4638	*S. aureus* ClpP	MT4637	This study
MT4639	Human proClpP	MT4637	This study
MT4640	Human proClpP mutant	MT4637	This study
MT4641	Human ClpP	MT4637	This study

shRNA sequences:
> shRNA CLPP - 46858: CCGGGCTCTATAACATCTACGCCAACTCGAGTTGGCGTAGATGTTATAGAGCTTTTTG
> shRNA CLPP – 46859 CCGGGCCCATCCACATGTACATCAACTCGAGTTGATGTACATGTGGATGGGCTTTTTG
>shRNA CLPP - 46860: CCGGGCTCAAGAAGCAGCTCTATAACTCGAGTTATAGAGCTGCTTCTTGAGCTTTTTG
> shRNA CLPP - 46861: CCGGCACGATGCAGTACATCCTCAACTCGAGTTGAGGATGTACTGCATCGTGTTTTTG
>shRNA CLPP - 46862: CCGGGTTTGGCATCTTAGACAAGGTCTCGAGACCTTGTCTAAGATGCCAAACTTTTTG
sgRNA guide sequences:
> CLPP-1: GGATCATGATACGGGAGTTG
> CLPP-2: GCGCCTATGACATCTACTCG
> CLPP-3: GAGCGAGTGGCGCATGCCTG

> MIPEP-1: GCCAGCATTCAGAGAAGCTG
> MIPEP-2: TAGCACCATACCCCACGAGG
> MIPEP-3: CAGCACCAGCTGGTCTCCCG
> AAVS1: GGGGCCACTAGGGACAGGAT
>Azami-green: GGCCACAACTTCGTGATCGA
DNA sequence of yeast expression plasmids and CLPP/ClpP variants:
>MT4637|expression vector: TGGTAAATAGAAACGGAACTTTACATATTGAATACCGGAGATATAATTCGTTTATGCCACATAATCAT CAATACATCCGTAACCCGCCCGAAACGGAAAAACTGAAGAAAAAGCATCTGTGCGGTATTTCACACC GCATATGATCCGTCGAGTTCAAGAGAAAAAAAAAGAAAAAGCAAAAAGAAAAAAGGAAAGCGCGCC TCGTTCAGAATGACACGTATAGAATGATGCATTACCTTGTCATCTTCAGTATCATACTGTTCGTATACA TACTTACTGACATTCATAGGTATACATATATACACATGTATATATATCGTATGCTGCAGCTTTAAATAAT CGGTGTCACTACATAAGAACACCTTTGGTGGAGGGAACATCGTTGGTACCATTGGGCGAGGTGGCTT CTCTTATGGCAACCGCAAGAGCCTTGAACGCACTCTCACTACGGTGATGATCATTCTTGCCTCGCAGA CAATCAACGTGGAGGGTAATTCTGCTAGCCTCTGCAAAGCTTTCAAGAAAATGCGGGATCATCTCGCA AGAGAGATCTCCTACTTTCTCCCTTTGCAAACCAAGTTCGACAACTGCGTACGGCCTGTTCGAAAGATC TACCACCGCTCTGGAAAGTGCCTCATCCAAAGGCGCAAATCCTGATCCAAACCTTTTTACTCCACGCGC CAGTAGGGCCTCTTTAAAAGCTTGACCGAGAGCAATCCCGCAGTCTTCAGTGGTGTGATGGTCGTCTA TGTGTAAGTCACCAATGCACTCAACGATTAGCGACCAGCCGGAATGCTTGGCCAGAGCATGTATCATA TGGTCCAGAAACCCTATACCTGTGTGGACGTTAATCACTTGCGATTGTGTGGCCTGTTCTGCTACTGCT TCTGCCTCTTTTTCTGGGAAGATCGAGTGCTCTATCGCTAGGGGACCACCCTTTAAAGAGATCGCAAT CTGAATCTTGGTTTCATTTGTAATACGCTTTACTAGGGCTTTCTGCTCTGTCATCTTTGCCTTCGTTTATC TTGCCTGCTCATTTTTTAGTATATTCTTCGAAGAAATCACATTACTTTATATAATGTATAATTCATTATGT GATAATGCCAATCGCTAAGAAAAAAAAAGAGTCATCCGCTAGGTGGAAAAAAAAAAATGAAAATCAT TACCGAGGCATAAAAAAATATAGAGTGTACTAGAGGAGGCCAAGAGTAATAGAAAAAGAAAATTGC GGGAAAGGACTGTGTTATGACTTCCCTGACTAATGCCGTGTTCAAACGATACCTGGCAGTGACTCCTA GCGCTCACCAAGCTCTTAAAACGGAATTATGGTGCACTCTCAGTACAATCTGCTCTGATGCCGCATAG TTAAGCCAGCCCCGACACCCGCCAACACCCGCTGACGCGCCCTGACGGGCTTGTCTGCTCCCGGCATC CGCTTACAGACAAGCTGTGACCGTCTCCGGGAGCTGCATGTGTCAGAGGTTTTCACCGTCATCACCGA AACGCGCGAGACGAAAGGGCCTCGTGATACGCCTATTTTTATAGGTTAATGTCATGATAATAATGGTT TCTTAGGACGGATCGCTTGCCTGTAACTTACACGCGCCTCGTATCTTTTAATGATGGAATAATTTGGGA ATTTACTCTGTGTTTATTTATTTTTATGTTTTGTATTTGGATTTTAGAAAGTAAATAAAGAAGGTAGAA GAGTTACGGAATGAAGAAAAAAAAAATAAACAAAGGTTTAAAAAATTTCAACAAAAAGCGTACTTTAC ATATATATTTATTAGACAAGAAAAGCAGATTAAATAGATATACATTCGATTAACGATAAGTAAAATGT AAAATCACAGGATTTTCGTGTGTGGTCTTCTACACAGACAAGATGAAACAATTCGGCATTAATACCTG AGAGCAGGAAGAGCAAGATAAAAGGTAGTATTTGTTGGCGATCCCCCTAGAGTCTTTTACATCTTCG GAAAACAAAAACTATTTTTTCTTTAATTTCTTTTTTTACTTTCTATTTTTAATTTATATATTTATATTAAAA AATTTAAATTATAATTATTTTTATAGCACGTGATGAAAAGGACCCAGGTGGCACTTTTCGGGGAAATG

TGCGCGGAACCCCTATTTGTTTATTTTTCTAAATACATTCAAATATGTATCCGCTCATGAGACAATAACC
CTGATAAATGCTTCAATAATATTGAAAAAGGAAGAGTATGAGTATTCAACATTTCCGTGTCGCCCTTAT
TCCCTTTTTTGCGGCATTTTGCCTTCCTGTTTTTGCTCACCCAGAAACGCTGGTGAAAGTAAAAGATGC
TGAAGATCAGTTGGGTGCACGAGTGGGTTACATCGAACTGGATCTCAACAGCGGTAAGATCCTTGAG
AGTTTTCGCCCCGAAGAACGTTTTCCAATGATGAGCACTTTTAAAGTTCTGCTATGTGGCGCGGTATTA
TCCCGTATTGACGCCGGGCAAGAGCAACTCGGTCGCCGCATACACTATTCTCAGAATGACTTGGTTGA
GTACTCACCAGTCACAGAAAAGCATCTTACGGATGGCATGACAGTAAGAGAATTATGCAGTGCTGCC
ATAACCATGAGTGATAACACTGCGGCCAACTTACTTCTGACAACGATCGGAGGACCGAAGGAGCTAA
CCGCTTTTTTTCACAACATGGGGGATCATGTAACTCGCCTTGATCGTTGGGAACCGGAGCTGAATGAA
GCCATACCAAACGACGAGCGTGACACCACGATGCCTGTAGCAATGGCAACAACGTTGCGCAAACTAT
TAACTGGCGAACTACTTACTCTAGCTTCCCGGCAACAATTAATAGACTGGATGGAGGCGGATAAAGTT
GCAGGACCACTTCTGCGCTCGGCCCTTCCGGCTGGCTGGTTTATTGCTGATAAATCTGGAGCCGGTGA
GCGTGGGTCTCGCGGTATCATTGCAGCACTGGGGCCAGATGGTAAGCCCTCCCGTATCGTAGTTATCT
ACACGACGGGCAGTCAGGCAACTATGGATGAACGAAATAGACAGATCGCTGAGATAGGTGCCTCAC
TGATTAAGCATTGGTAACTGTCAGACCAAGTTTACTCATATATACTTTAGATTGATTTAAAACTTCATTT
TTAATTTAAAAGGATCTAGGTGAAGATCCTTTTTGATAATCTCATGACCAAAATCCCTTAACGTGAGTT
TTCGTTCCACTGAGCGTCAGACCCCGTAGAAAAGATCAAAGGATCTTCTTGAGATCCTTTTTTTCTGCG
CGTAATCTGCTGCTTGCAAACAAAAAAACCACCGCTACCAGCGGTGGTTTGTTTGCCGGATCAAGAGC
TACCAACTCTTTTTCCGAAGGTAACTGGCTTCAGCAGAGCGCAGATACCAAATACTGTCCTTCTAGTGT
AGCCGTAGTTAGGCCACCACTTCAAGAACTCTGTAGCACCGCCTACATACCTCGCTCTGCTAATCCTGT
TACCAGTGGCTGCTGCCAGTGGCGATAAGTCGTGTCTTACCGGGTTGGACTCAAGACGATAGTTACC
GGATAAGGCGCAGCGGTCGGGCTGAACGGGGGGTTCGTGCACACAGCCCAGCTTGGAGCGAACGA
CCTACACCGAACTGAGATACCTACAGCGTGAGCATTGAGAAAGCGCCACGCTTCCCGAAGGGAGAAA
GGCGGACAGGTATCCGGTAAGCGGCAGGGTCGGAACAGGAGAGCGCACGAGGGAGCTTCCAGGGG
GGAACGCCTGGTATCTTTATAGTCCTGTCGGGTTTCGCCACCTCTGACTTGAGCGTCGATTTTTGTGAT
GCTCGTCAGGGGGGCCGAGCCTATGGAAAAACGCCAGCAACGCGGCCTTTTTACGGTTCCTGGAAAA
TGTATTAATAAATAAAAGAACTTAAATATAGACTTTTTATTCGCATGCATATAAAAATAATTAATTAAT
AAATAACTGTAAAAAACTAGAATAATAAAAGTAATAAATATCTCCTCCGACGACATAGCTTTTGAGGG
AATATTCAACTGTTTTTTTTTATCATGTTGATGCTCTGCATAATAATGCCCATAAATATTTCCGACCTGC
TTTTATATCTTTGCTAGCCAAACTAACTGAACATAGCTACACATTATTTTCAGCTTGGCTATTTTGTGAA
CACTGTATAGCCAGTCCTTCGGATCACGGTCAACAGTTGTCCGAGCGCTTTTTGGACCCTTTCCCTTAT
TTTTGGGTTAAGGAAAATGACAGAAAATATATCTAATGAGCCTTCGCTCAACAGTGCTCCGAAGTATA
GCTTTCCAAAAGGAGAGGCAAAGCAATTTAAGAATGTATGAACAAAATAAAGGGGAAAAATTACCCC
CTCTACTTTACCAAACGAATACTACCAATAATATTTACAACTTTTCCTTATGATTTTTTCACTGAAGCGC
TTCGCAATAGTTGTGAGTGATATCAAAAGTAACGAAATGAACTCCGCGGCTCGTGCTATATTCTTGTT
GCTACCGTCCATATCTTTCCATAGATTTTCAATTTTTGATGTCTCCATGGTGGTACAGAGAACTTGTAA
ACAATTCGGTCCCTACATGTGAGGAAATTCGCTGTGACACTTTTATCACTGAACTCCAAATTTAAAAAA
TAGCATAAAATTCGTTATACAGCAAATCTATGTGTTGCAATTAAGAACTAAAAGATATAGAGTGCATA
TTTTCAAGAAGGATAGTAAGCTGGCAAAGGACCATTGCTGAATCACAAATTCTCTCCACTTCCTTATTT
TCCTTCATATAATAAGACATAAAAAACTTGTATATTATTAGGTATTTAGCTCGTTTTCAAAAATTCTTAC
TTTTTTTTTGGATGGACGCAAAGAAGTTTAATAATCATATTACATGGCATTACCACCATATACATATCC
ATATACATATCCATATCTAATCTTACTTATATGTTGTGGAAATGTAAAGAGCCCCATTATCTTAGCCTAA
AAAAACCTTCTCTTTGGAACTTTCAGTAATACGCTTAACTGCTCATTGCTATATTGAAGTACGGATTAG
AAGCCGCCGAGCGGGCGACAGTCCTCCGACGGAAGACTCTCCTCCGTGCGTCCTCGTCTTCACCGGTC

GCGTTCCTGAAACGCAGATGTGCCTCGCGCCGCACTGCTCCGAACAATAAAGATTCTACAATACTAGC
TTTTATGGTTATGAAGAGGAAAAATTGGCAGTAACCTGGCCCCACAAACCTTCAAATTAACGAATCAA
ATTAACAACCATAGGATGATAATGCGATTAGTTTTTTAGCCTTATTTCTGGGGTAATTAATCAGCGAAG
CGATGATTTTTGATCTATTAACAGATATATAAATGGAAAAGCTGCATAACCACTTTAACTAATACTTTC
AACATTTTCAGTTTGTATTACTTCTTATTCAAATGTCATAAAAGTATCAACAAAAAATTGTTAATATACC
TCTATACTTTAACGTCAAGGAGAAAAAACCC

> MT4638|*S. aureus* ClpP:
ATGAATTTAATTCCTACAGTTATTGAAACAACAAACCGTGGTGAAAGAGCATATGACATCTATTCGAG
GTTATTGAAGGACCGTATCATCATGCTGGGTTCACAAATAGATGACAACGTCGCCAATTCAATCGTGA
GCCAGCTTCTCTTTTTGCAGGCCCAAGACTCTGAGAAAGACATCTACCTTTACATTAATTCACCAGGTG
GAAGTGTAACGGCTGGTTTTGCAATTTACGACACTATCCAGCATATAAAGCCGGACGTTCAAACAATT
TGTATCGGTATGGCAGCATCAATGGGATCATTCTTATTAGCAGCTGGTGCAAAAGGTAAAAGGTTCG
CGTTACCAAATGCAGAAGTAATGATTCACCAACCATTAGGTGGCGCCCAAGGACAAGCCACTGAGAT
CGAGATCGCCGCCAACCACATTCTAAAAACCAGGGAGAAATTGAATAGAATCCTATCGGAGAGGACC
GGACAATCGATTGAGAAGATTCAAAAAGATACCGACAGAGACAATTTCCTCACTGCAGAAGAAGCTA
AGGAATATGGCCTAATTGATGAAGTGATGGTACCTGAAACAAAATAA

> MT4639|human proCLPP:
ATGTGGCCGGGAATACTTGTCGGTGGAGCACGTGTTGCTTCATGCAGATATCCAGCTTTAGGTCCACG
CCTAGCAGCTCATTTTCCAGCACAACGACCACCACAGAGGACACTCCAGAATGGTTTAGCCTTGCAGA
GGTGTTTACATGCCACAGCTACTAGAGCTTTGCCTTTAATCCCAATAGTGGTGGAACAAACGGGTCGA
GGCGAGCGGGCTTATGACATTTACTCGAGACTGTTAAGAGAACGTATCGTCTGTGTCATGGGCCCGA
TCGACGATAGCGTTGCCAGCCTTGTTATCGCACAGCTTCTGTTCCTGCAATCCGAGAGCAATAAAAAG
CCCATCCACATGTACATCAACTCTCCTGGTGGTGTAGTAACAGCTGGCCTGGCCATCTATGATACGAT
GCAGTACATCCTCAATCCAATATGTACCTGGTGCGTGGGCCAGGCTGCATCAATGGGCAGTCTATTAT
TAGCAGCCGGCACTCCAGGTATGCGCCATTCTTTGCCAAACAGCAGGATTATGATCCATCAACCATCT
GGTGGAGCAAGAGGCCAAGCCACAGACATTGCCATCCAGGCAGAGGAGATCATGAAGCTCAAGAAG
CAGCTCTATAACATCTACGCCAAGCACACCAAACAGAGTTTACAGGTGATTGAATCCGCCATGGAGA
GGGACCGCTATATGTCACCAATGGAAGCGCAGGAGTTTGGCATCTTAGACAAGGTTTTAGTTCATCCA
CCTCAAGACGGGGAGGATGAGCCCACACTTGTACAAAAGGAGCCGGTCGAAGCAGCGCCGGCCGCA
GAGCCTGTTCCAGCTAGCACCTGA

> MT4641|human CLPP:
ATGCCTTTAATCCCAATAGTGGTGGAACAAACGGGTCGAGGCGAGCGGGCTTATGACATTTACTCGA
GACTGTTAAGAGAACGTATCGTCTGTGTCATGGGCCCGATCGACGATAGCGTTGCCAGCCTTGTTATC
GCACAGCTTCTGTTCCTGCAATCCGAGAGCAATAAAAAGCCCATCCACATGTACATCAACTCTCCTGGT
GGTGTAGTAACAGCTGGCCTGGCCATCTATGATACGATGCAGTACATCCTCAATCCAATATGTACCTG
GTGCGTGGGCCAGGCTGCATCAATGGGCAGTCTATTATTAGCAGCCGGCACTCCAGGTATGCGCCAT
TCTTTGCCAAACAGCAGGATTATGATCCATCAACCATCTGGTGGAGCAAGAGGCCAAGCCACAGACA
TTGCCATCCAGGCAGAGGAGATCATGAAGCTCAAGAAGCAGCTCTATAACATCTACGCCAAGCACAC
CAAACAGAGTTTACAGGTGATTGAATCCGCCATGGAGAGGGACCGCTATATGTCACCAATGGAAGCG
CAGGAGTTTGGCATCTTAGACAAGGTTTTAGTTCATCCACCTCAAGACGGGGAGGATGAGCCCACAC
TTGTACAAAAGGAGCCGGTCGAAGCAGCGCCGGCCGCAGAGCCTGTTCCAGCTAGCACCTGA

> MT4640|human proCLPP mutant:
ATGTGGCCGGGAATACTTGTCGGTGGAGCACGTGTTGCTTCATGCAGATATCCAGCTTTAGGTCCACG
CCTAGCAGCTCATTTTCCAGCACAACGACCACCACAGAGGACACTCCAGAATGGTTTAGCCTTGCAGA

GGTGTGATTTTGCCCTAGCTCTACTATGTTTGCCTTTAATCCCAATAGTGGTGGAACAAACGGGTCGA
GGCGAGCGGGCTTATGACATTTACTCGAGACTGTTAAGAGAACGTATCGTCTGTGTCATGGGCCCGA
TCGACGATAGCGTTGCCAGCCTTGTTATCGCACAGCTTCTGTTCCTGCAATCCGAGAGCAATAAAAAG
CCCATCCACATGTACATCAACTCTCCTGGTGGTGTAGTAACAGCTGGCCTGGCCATCTATGATACGAT
GCAGTACATCCTCAATCCAATATGTACCTGGTGCGTGGGCCAGGCTGCATCAATGGGCAGTCTATTAT
TAGCAGCCGGCACTCCAGGTATGCGCCATTCTTTGCCAAACAGCAGGATTATGATCCATCAACCATCT
GGTGGAGCAAGAGGCCAAGCCACAGACATTGCCATCCAGGCAGAGGAGATCATGAAGCTCAAGAAG
CAGCTCTATAACATCTACGCCAAGCACACCAAACAGAGTTTACAGGTGATTGAATCCGCCATGGAGA
GGGACCGCTATATGTCACCAATGGAAGCGCAGGAGTTTGGCATCTTAGACAAGGTTTTAGTTCATCCA
CCTCAAGACGGGGAGGATGAGCCCACACTTGTACAAAAGGAGCCGGTCGAAGCAGCGCCGGCCGCA
GAGCCTGTTCCAGCTAGCACCTGA

Note: Full plasmid DNA sequences of MT4638, MT4639, MT4640 and MT4641 can be obtained by appending the ClpP insert DNA sequence 5'end of the MT4637 expression vector sequence. Full plasmid DNA sequences for shRNA and sgRNA constructs can be obtained by placing the inserts in the appropriate insertion sites of pLKO.1-puro and lentiCRISPRv2GFP, respectively.

Supplementary Table S6. *Saccharomyces cerevisiae* strains used in this study.

strain	genotype	source
S288C BY4741 (MT1448)	*MAT***a** *his3Δ1 leu2Δ0 met15Δ0 ura3Δ0*	BRACHMANN *et al.* 1998
S288C BY4741 *oct1Δ* (MT5034)	*MAT***a** *his3Δ1 leu2Δ0 met15Δ0 ura3Δ0, oct1::KanMX*	Euroscarf, Y04984
Y13206 (MT5035)	*MATα pdr1Δ::natMX, pdr3Δ::KI.URA3, snq2Δ::KI.LEU2*	PIOTROWSKI *et al.* 2017

Supplementary Table S7. Bacterial strains used in this study.

bacterial strain	identifier	source
Escherichia coli Stbl3	C737303	ThermoFisher Scientific
Escherichia coli BW25113	none	Gerard D. Wright lab
Escherichia BW25113 ΔbamBΔtolC	none	KING *et al.* 2014
Bacillus subtilis 168	ATCC23857	Gerard D. Wright lab
Bacillus subtilis 168 ΔclpP::spc	none	MSADEK *et al.* 1998
Staphylococcus aureus	ATCC29213	Gerard D. Wright lab
Neisseria gonorrhoeae	WHOY	Gerard D. Wright lab
Neisseria gonorrhoeae	ATCC49226	Gerard D. Wright lab
Enterococcus faecium	ATCC19434	Gerard D. Wright lab
Klebsiella pneumonia	ATCC33495	Gerard D. Wright lab
Acinetobacter baumannii	ATCC17978	Gerard D. Wright lab
Pseudomonas aeruginosa	PA01	Gerard D. Wright lab
Enterobacter aerogenes	ATCC13048	Gerard D. Wright lab
Mycobacterium tuberculosis H37Ra	ATCC 25177	Gerard D. Wright lab
Mycobacterium smegmatis	mc2155	Gerard D. Wright lab

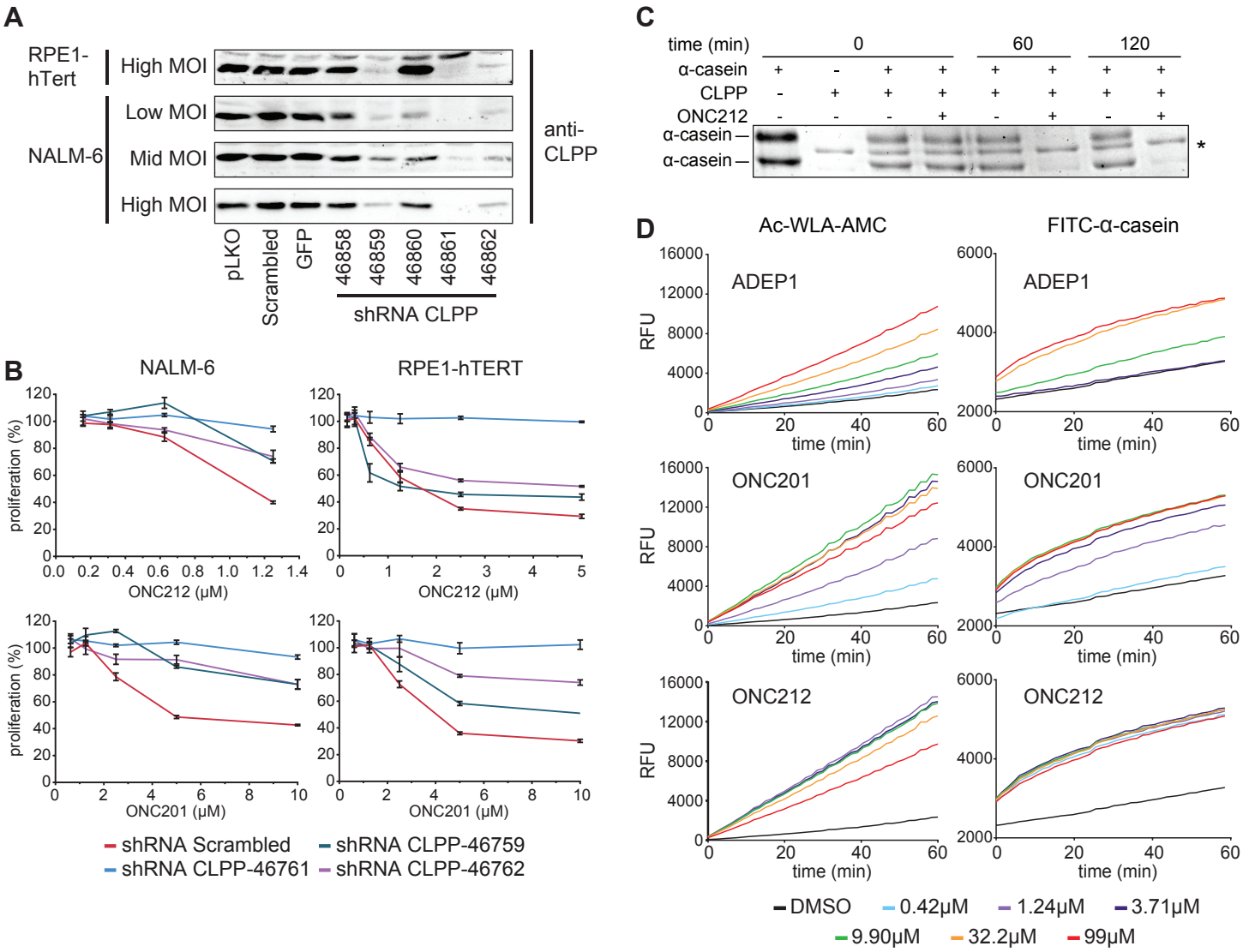

Supplementary Figure 1. Validation of CRISPR screen hits. **A.** Immunoblot analysis of CLPP protein levels in NALM6 or RPE1-hTert populations transduced with the indicated CLPP shRNA constructs. **B.** Cell proliferation of knockdown populations of NALM-6 or RPE1-hTert cells transduced with constructs either expressing control (scrambled) or CLPP shRNAs and treated for 72 h with the indicated concentrations of ONC212. Cell number was assessed by bioluminescent quantitation of cellular ATP levels normalized to culture volume. Proliferation is shown as mean ± SD (n=12, 3 biological replicates) relative to solvent (0.1% DMSO) controls. **C.** Degradation of full length unlabelled α-casein by purified recombinant human CLPP in the presence of 100 μM ONC212 or 0.1% DMSO control. Proteins were resolved by SDS-PAGE and detected by Coomassie Brilliant Blue strain. Asterisk denotes input recombinant CLPP. **D.** Effects of ADEP1, ONC201 and ONC212 on degradation of fluorescent Ac-WLA-AMC peptide and FITC-α-casein substrates by purified recombinant human CLPP. Relative luminescent unit (RLU) values are the mean of triplicate measurements. For unknown reasons, at the highest concentration used (0.1 mM) both ONC201 and ONC212 interfered with activity against the peptide substrate but not the protein substrate.

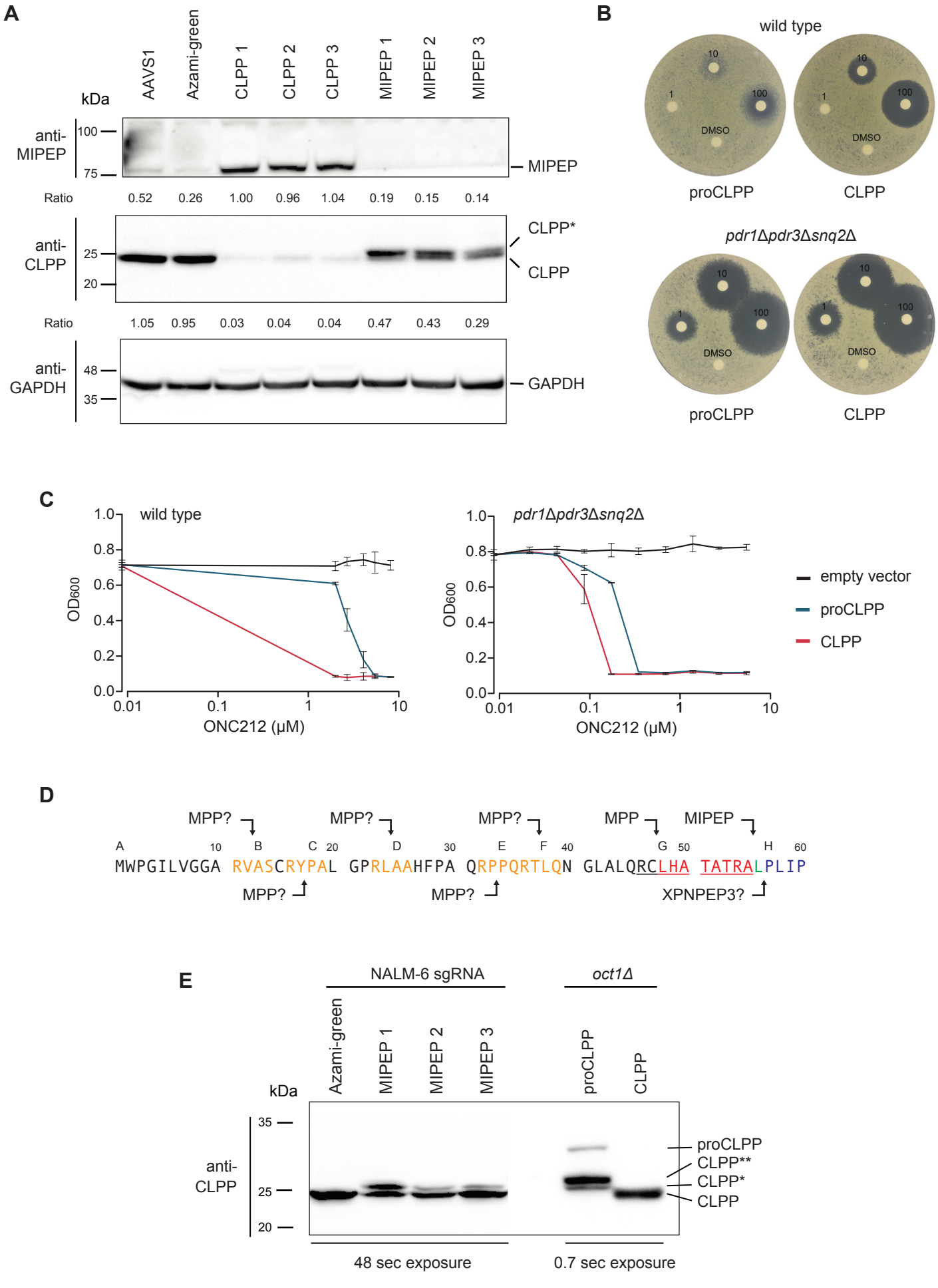
A
AAVS1
Azami-green
CLPP 1
CLPP 2
CLPP 3
MIPEP 1
MIPEP 2
MIPEP 3
kDa
anti-MIPEP
100
75
MIPEP
Ratio
0.52 0.26 1.00 0.96 1.04 0.19 0.15 0.14
anti-CLPP
25
20
CLPP*
CLPP
Ratio
1.05 0.95 0.03 0.04 0.04 0.47 0.43 0.29
anti-GAPDH
48
35
GAPDH
B
wild type
10
1
100
DMSO
proCLPP
CLPP
pdr1Δpdr3Δsnq2Δ
C
wild type
pdr1Δpdr3Δsnq2Δ
OD600
ONC212 (μM)
empty vector
proCLPP
CLPP
D
MPP?
MPP?
MPP?
MPP
MIPEP
MWPGILVGGA RVASCRYPAL GPRLAAHFPA QRPPQRTLQN GLALQRCLHA TATRALPLIP
MPP?
MPP?
XPNPEP3?
E
NALM-6 sgRNA
oct1Δ
Azami-green
MIPEP 1
MIPEP 2
MIPEP 3
proCLPP
CLPP
kDa
anti-CLPP
35
25
20
proCLPP
CLPP**
CLPP*
CLPP
48 sec exposure
0.7 sec exposure

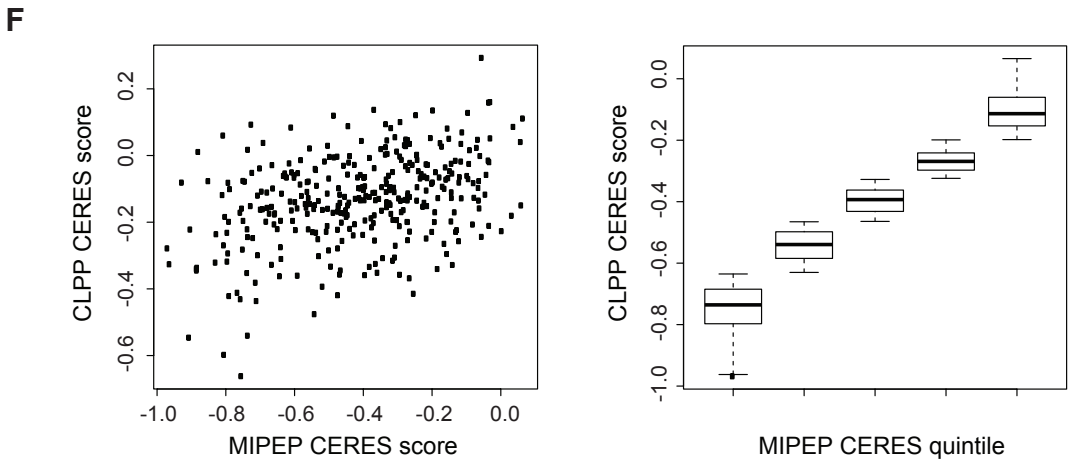

Supplementary Figure 2. Processing of human proCLPP by mitochondrial proteases. **A.** Immunoblot analysis of CLPP, MIPEP and GAPDH protein levels in NALM6 cell line knockout populations for indicated control (AAVS1, Azami-Green), CLPP and MIPEP sgRNAs. Knockout populations were generated as in panel 1F followed by selection in 150 nM ONC212 for the final 3 days of growth. CLPP and MIPEP ratios determined by densitometry and normalized to the average of AAVS1 and Azami-Green controls for CLPP or the average of the CLPP knockout population for MIPEP. **B.** Disk diffusion assay of wild type or efflux pump deficient (*pdr1*Δ*pdr3*Δ*snq2*Δ) *S. cerevisiae* strains that expressed either mature human CLPP or proCLPP from the *GAL1* promoter. Disks contained either 0, 1, 10 or 100 nmol of ONC212. SC-Leu medium plates containing 2% galactose were incubated at 30°C for 2 days. **C.** Proliferation of wild type or efflux pump deficient S. cerevisiae strains that expressed either mature human CLPP or proCLPP from the *GAL1* promoter or empty vector control. Cells were grown in the indicated concentration of ONC212 for 48 h and cell density determined by OD_{600}. Data are the mean of triplicate samples ± SD. **D.** Processing motifs and cleavage sites in the N-terminal region of CLPP. Residues 1-60 of unprocessed proCLPP are shown. Full length proCLPP (residues 1-277) has a predicted Mr of 30.2 kDa (fragment A) and mature CLPP (amino acids 57-277) has a predicted Mr of 24.2 kDa (fragment H). The CLPP* species observed in NALM-6 cells and *S. cerevisiae* correspond to mature CLPP with an unprocessed N-terminal octapeptide (shown in red) due to inactivation of MIPEP or its yeast ortholog Oct1, respectively (Fig. 2D and Supplemental Fig. 2E). This partially processed CLPP fragment (residues 48-277) has a predicted Mr of 25.1 kDa (fragment G). The CLPP** species observed in the *oct1Δ* yeast strain is likely due to MPP cleavage at one of the putative MPP R-2 cleavage motifs (shown in orange) present upstream of the MPP/MIPEP R-10 motif (Gakh *et al.* 2002). This cleavage would generate one of the CLPP fragments B-F, with fragment D (amino acid 25-277) the most likely candidate with a predicted Mr of 27.7 kDa. Sequential processing by MPP of propeptides with more than one MPP consensus site has been observed previously in yeast (Dasari and Kolling 2016). Predicted processing enzyme cleavage sites are indicated by arrows. The R-10 motif sequentially cleaved by MPP and MIPEP is underlined. The remaining Leu after MIPEP cleavage is removed by XPNEP3 or its yeast ortholog Icp55, or a similar aminopeptidase and is shown in green. The first residues of mature CLPP are shown in blue. **E.** Co-migration of CLPP isoforms produced in NALM-6 knockout populations for MIPEP versus in an *S. cerevisiae oct1*Δ mutant that expressed either human mature CLPP or proCLPP. Samples were resolved in adjacent lanes of a single SDS-PAGE gel prior to immunoblot detection.Two exposures were taken for comparison because much higher levels of each protein were produced in yeast. **F**. MIPEP and CLPP dependency scores in CRISPR loss-of-function essentiality screens across 341 cancer cell lines (Meyers *et al.* 2017). Left: scatterplot of MIPEP versus CLPP dependency scores (R=0.329). Right: Boxplot after binning MIPEP scores. Dependency scores were determined using the CERES algorithm (Doench *et al.* 2016; Meyers *et al.* 2017). Loss of function screen data was obtained from the Avana library dataset (https://depmap.org/ceres/).

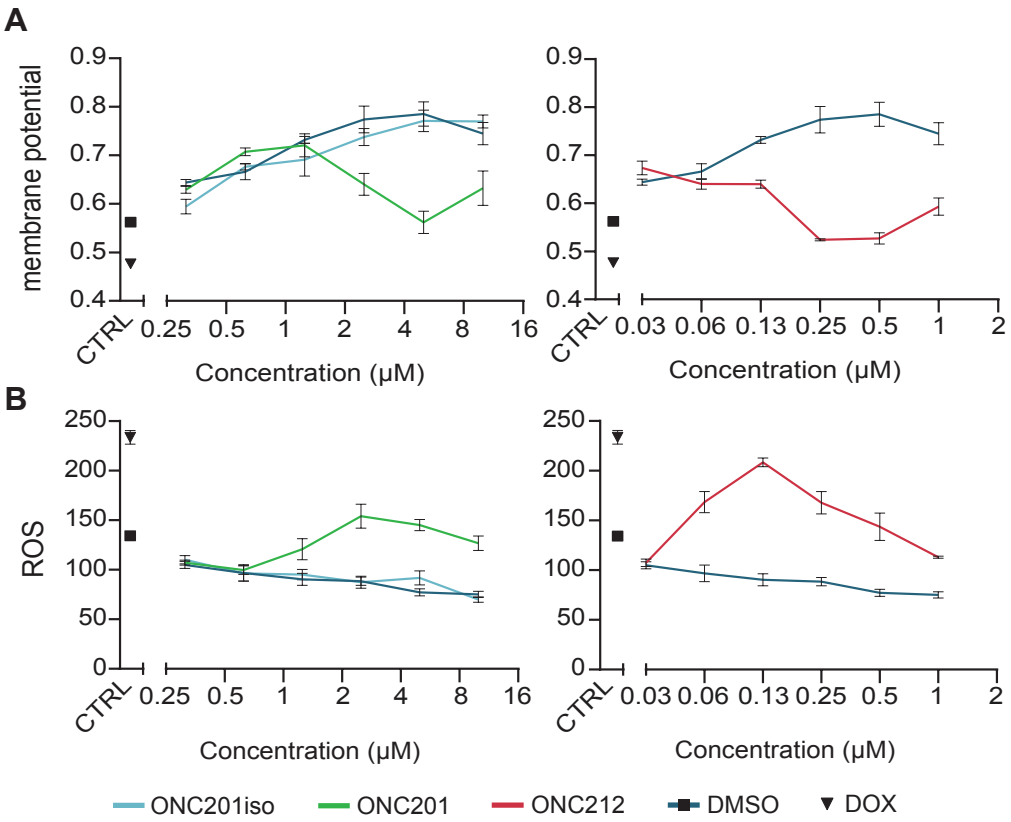

Supplementary Figure 3. Effect of ONC201 and ONC212 on mitochondrial function. **A.** Mitochondrial membrane potential was determined by membrane-potential sensitive dye incorporation. **B.** Mitochondrial reactive oxygen species (ROS) were determined by ROS-sensitive dye incorporation. NALM-6 cell cultures were treated for 3 days with the indicated concentrations of ONC201, ONC212 or with doxycycline (2 μM, 12 h) as a positive control, An inactive ONC201 isomer (TIC10iso) or solvent (0.1% DMSO) were used as negative controls. Results are expressed as mean value of triplicate samples ± SEM.

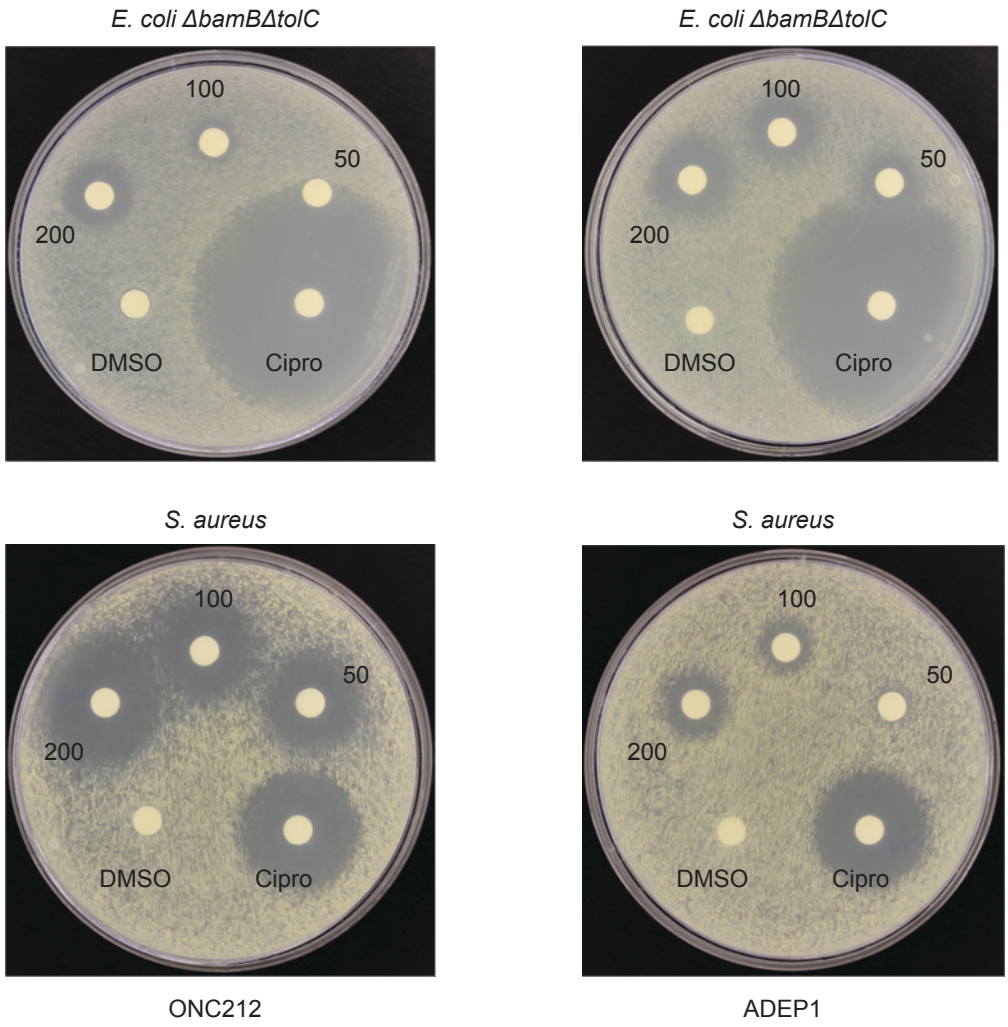

Supplementary Figure 4. Disk diffusion assays on *E. coli ΔbamBΔtolC* (top) and wild-type *S. aureus* (bottom). Disks contained either 50, 100 or 200 nmol of ONC212 (left) or ADEP1 (right). Ciprofloxacin (Cipro) at 2.7 nmol and DMSO were included as positive and negative controls, respectively. Plates were incubated at 37°C for 24 h.

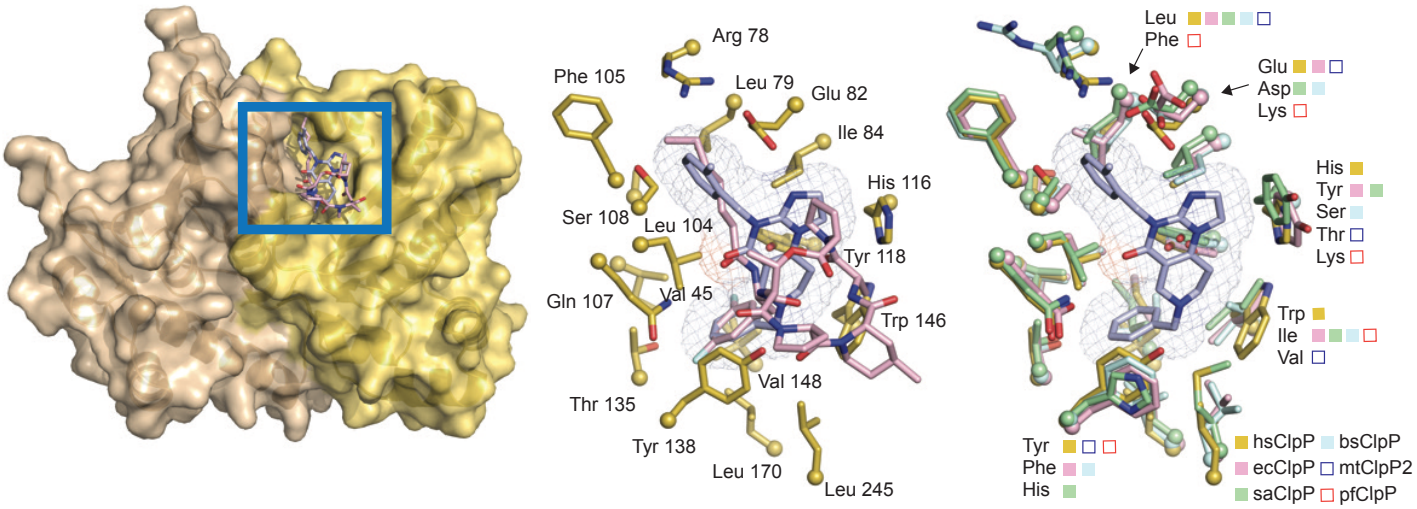

Supplementary Figure 5. Comparison of ADEP and imipridone binding modes in different species. Left: Surface rendered side-view of two adjacent ClpP monomers in complex with ONC201 and superimposed ADEP1. Middle: Expanded view of activator binding site. ONC201 is depicted in blue and ADEP1 is depicted in pink. Molecular volume of ONC201 is depicted in mesh. Based on structures 6DL7 (ISHIZAWA *et al.* 2019) and 6BBA (WONG *et al.* 2018) and previous analyses (ISHIZAWA *et al.* 2019; WONG AND HOURY 2019). Right: Activator binding site with residues of ClpP from multiple species superimposed. For clarity only ONC201 is depicted. Residues for each species are indicated by different colors. Open squares indicate residues for other species not shown in the structures. hs = *H. sapiens*; bs = *B. subtilis*; ec = *E. coli*; sa = *S. aureus*; mt = *M. tuberculosis*; pf = *P. falciparum*.

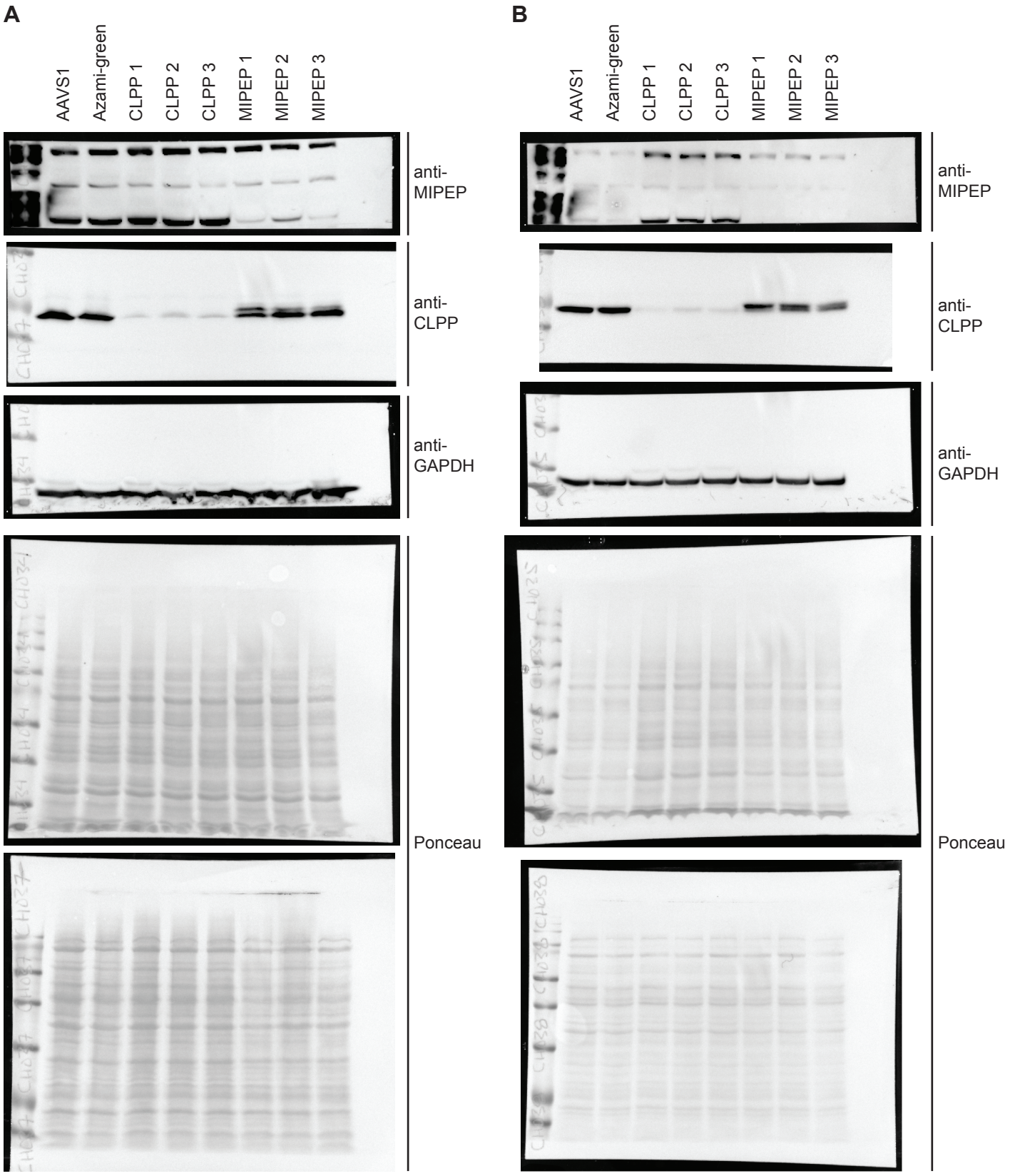

Supplementary Figure 6. Uncropped images corresponding to Figure 1F (panel A) and Suppl. Figure 2A (panel B).

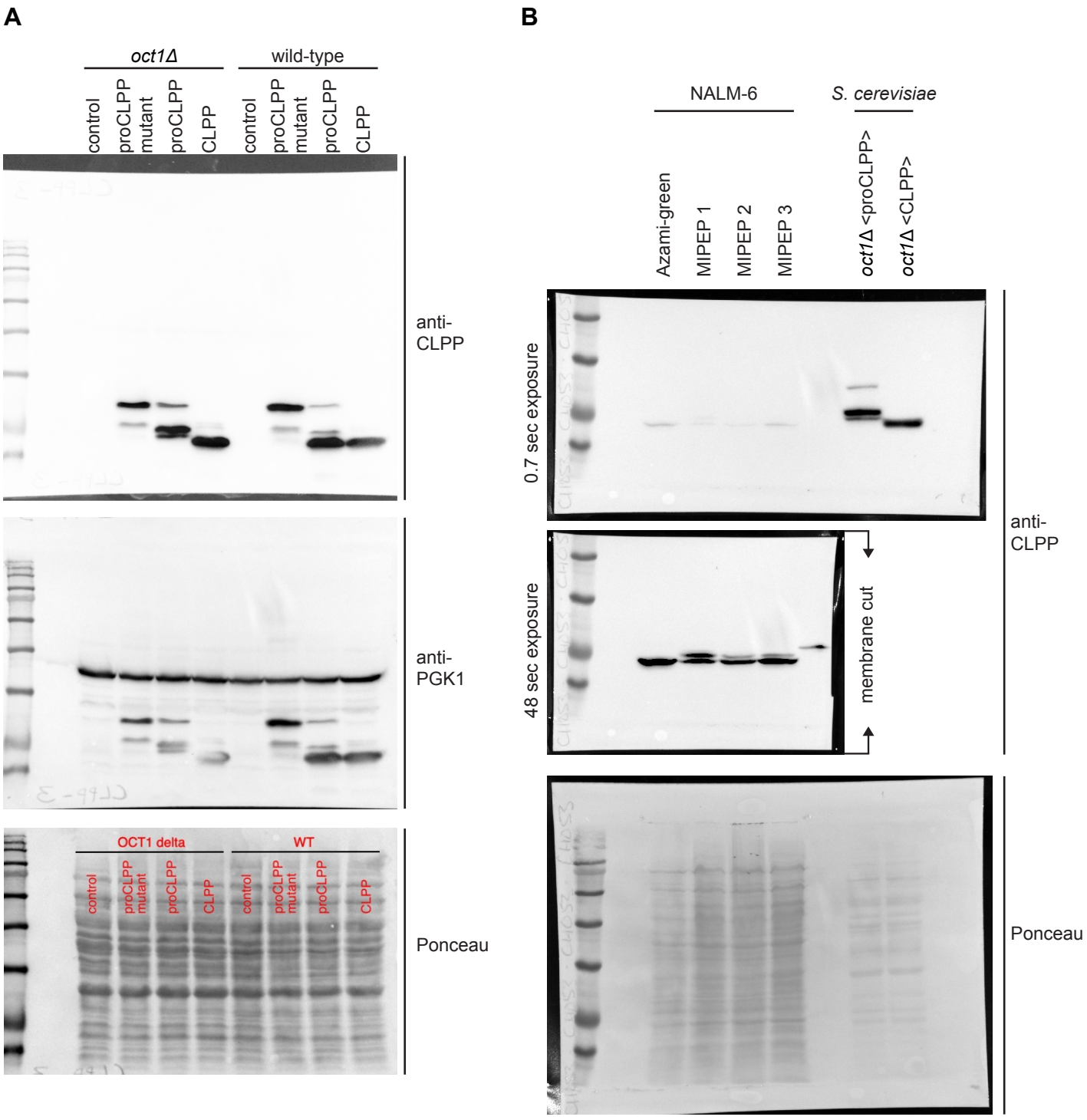

Supplementary Figure 7. Uncropped images corresponding to Figure 2D (panel A) and Suppl. Figure 2E (panel B).

A

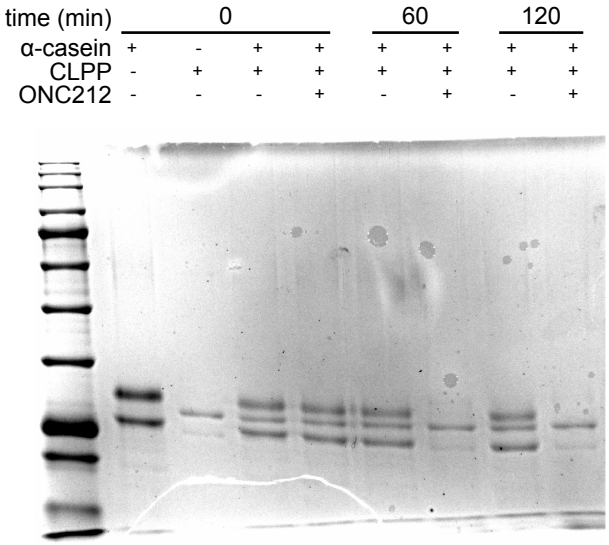

B

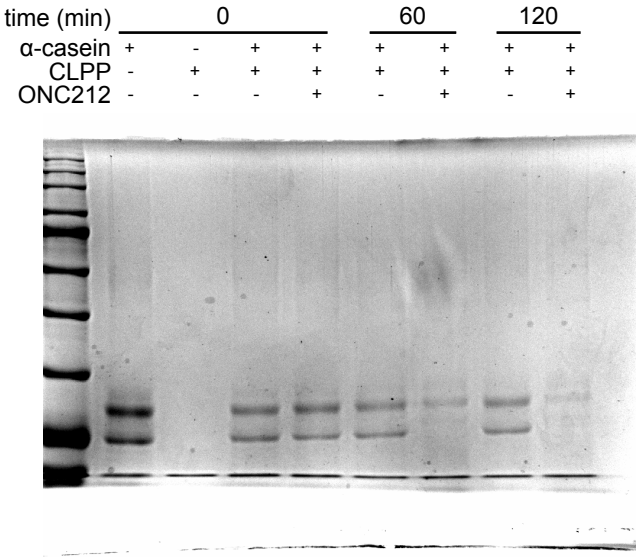

Supplementary Figure 8. Uncropped images corresponding to Suppl. Figure 1C (panel A) and Figure 4C (panel B).

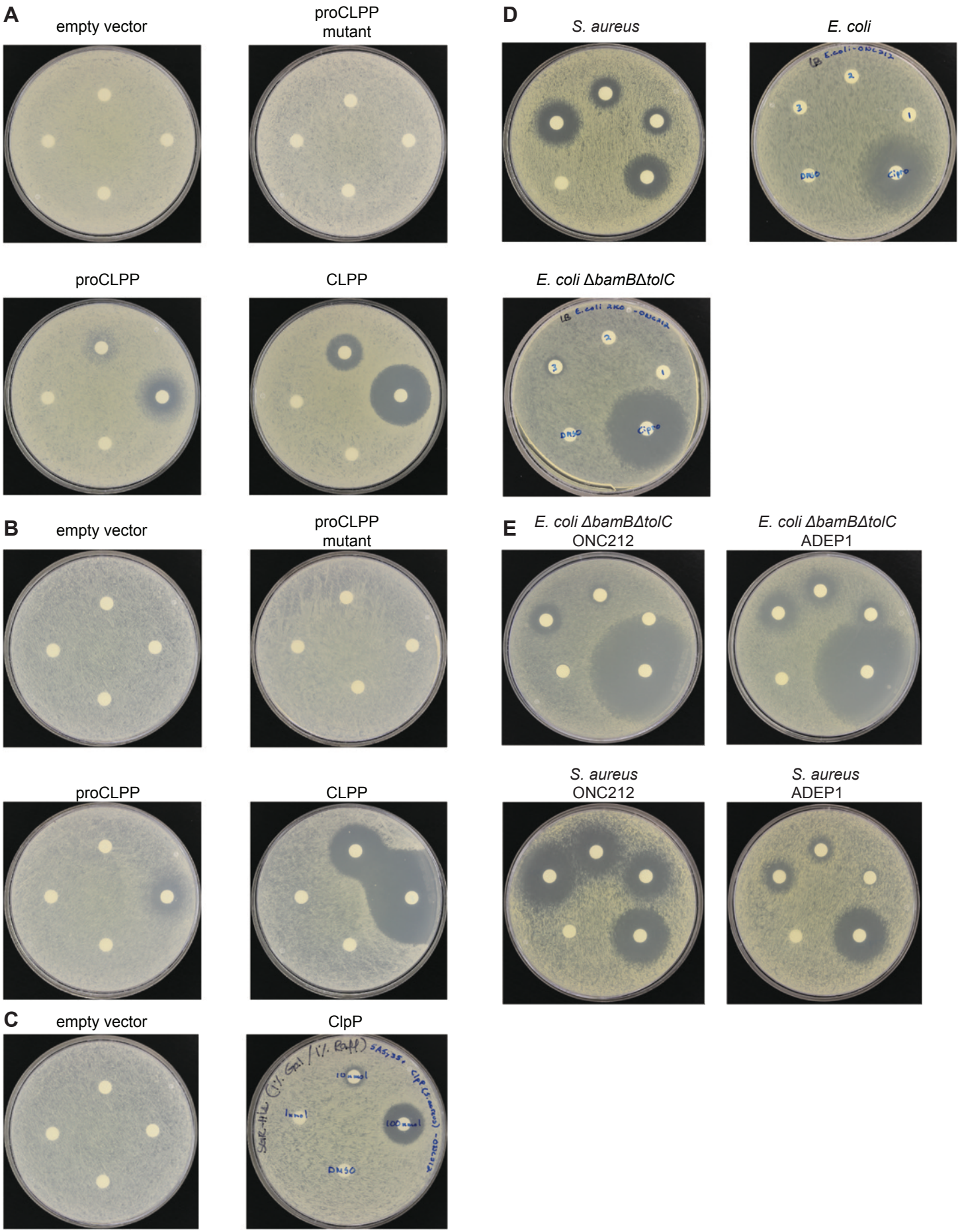

Supplementary Figure 9. Uncropped plate images with original contrast. Yeast plates correspond to Figure 2B (panel A), Figure 2C (panel B) and Figure 4A (panel C). Bacterial plates correspond to Figures 5B and D (panel D) and Suppl. Figure 4 (panel E).